Comparative Cardiac Anatomy

6

Alexander J. Hill and Paul A. Iaizzo

Abstract

The need for appropriate animal models to conduct translational research is vital for advancements in the diagnosis and treatment of heart disease. The choice of animal model to be employed must be critically evaluated. In this chapter, we present the comparative cardiac anatomies of several of the commonly employed animal models for preclinical research (dog, pig, and sheep). General comparisons focus on several specific anatomical features: the atria, ventricles, valves, coronary system, lymphatics, and the conduction system. Finally, we present novel qualitative and quantitative data obtained from perfusion-fixed specimens of these commonly used animal models.

Keywords

Comparative anatomy • Human • Sheep • Dog • Pig • Heart • Cardiac

6.1 Historical Perspective of Anatomy and Animal Research

Anatomy is one of the oldest branches of medicine, with historical records dating back at least as far as the third century BC; animal research dates back equally as far. More specifically, Aristotle (384–322 BC) studied comparative animal anatomy and physiology, and Erasistratus of Ceos (304–258 BC) studied live animal anatomy and physiology [1]. Galen of Pergamum (129–199 AD) is probably the most notable early anatomist who used animals in research in which he attempted to understand the normal structure and function of the body [2]. He continuously stressed the centrality of anatomy and made an attempt to dissect every day, as he felt it was critical to learning [3]. His most notable work was *De Anatomicis Administrationibus* (On Anatomical Procedures) which, when rediscovered in the sixteenth century, renewed interest in anatomy and scientific methods [2].

The Renaissance was a period of great scientific discovery and included important advances in our understanding of human and animal anatomy. Andreas Vesalius (1514–1564 AD) was arguably the greatest anatomist of the era [4]. To teach anatomy, he performed public nonhuman dissections at the University of Padua and is credited with creating the field of modern anatomy [2]. His immediate successors at Padua were Matteo Realdo Colombo (1510–1559 AD) and Gabriele Falloppio (1523–1562 AD). It was Colombo who, in great detail, described the pulmonary circulation and both the atrial and ventricular cavities; Falloppio is credited with the discovery of the Fallopian tubes among other things [4]. Animal research flourished during this period due to a number of popular ideas launched by both the Christian Church and one of the prominent scientific leaders at that time, Rene Descartes. The Church asserted that animals were under the dominion of man and, although worthy of respect, could be used to obtain information if it was for a "higher" purpose [2]. Descartes described humans and other animals as complex

A.J. Hill, PhD
Department of Surgery, University of Minnesota,
420 Delaware St. SE, B 172 Mayo, MMC 107,
Minneapolis, MN 55455, USA

Medtronic, 8200 Coral Sea Street NE, Mounds View,
MN 55112, USA

P.A. Iaizzo, PhD (✉)
Department of Surgery, University of Minnesota,
420 Delaware St. SE, B 172 Mayo, MMC 107,
Minneapolis, MN 55455, USA
e-mail: iaizz001@umn.edu

P.A. Iaizzo (ed.), *Handbook of Cardiac Anatomy, Physiology, and Devices*, DOI 10.1007/978-3-319-19464-6_6

machines, with the human soul distinguishing man from all other animals. This beast-machine concept was important for early animal researchers because if animals had no souls, it was thought that they could not suffer pain. Interestingly, it was believed that the reactions of animals were responses of automata and not pain [2].

The concept of functional biomedical studies can probably be attributed to another great scientist and anatomist, William Harvey (1578–1657 AD). He is credited with one of the most outstanding achievements in science and medicine—a demonstration of the circulation of blood which was documented in his publication *Exercitatio Anatomica De Motu Cordis et Sanguinis in Animalibus (De Motu Cordis)* in 1628. Very importantly, his work ushered in a new era in science, where a hypothesis was formulated and then tested through experimentation [4]. Many great anatomists emerged during this period and made innumerable discoveries; many of these discoveries were named after the individuals who described them and include several researchers who studied cardiac anatomy such as the Eustachian valve (Bartolomeo Eustachio), the Thebesian valve and Thebesian veins (Thebesius), and the sinus of Valsalva (Antonio Maria Valsalva). It should be noted that during this time period, in addition to animal research, dissections on deceased human bodies were performed, but not to the degree that they are today. In fact, it is written that, in general, during the post-Renaissance era, there was a serious lack of human bodies available for dissection. Oftentimes, bodies were obtained in a clandestine manner, by grave robbing or using bodies of executed criminals for dissection. In spite of the lack of bodies, most structures in the human body, including microscopic ones, were described by various anatomists and surgeons between the fifteenth and early nineteenth centuries.

Early in the nineteenth century, the first organized opposition to animal research occurred. In 1876, the Cruelty to Animals Act was passed in Britain. It was followed in the United States by the Laboratory Animal Welfare Act of 1966, which was amended in 1970, 1976, and 1985. These two acts began a new era in how laboratory animals were treated and utilized in experimental medicine. Importantly, the necessity of animal research is still great, and therefore animals continue to be used for a variety of purposes including cardiovascular device research.

6.2 Importance of Anatomy and Preclinical Animal Research

Anatomy remains as quite possibly one of the most important branches of medicine. In order to diagnose and treat medical conditions, normal structure and function must be known, as it is the basis for defining what is abnormal. Furthermore, structure typically has a great impact on the function of an organ, such as with the heart. For instance, a stenotic aortic valve will usually cause functional impairment of the left ventricle and lead to further pathologic conditions (e.g., ventricular hypertrophy). Thus, knowledge of anatomy and pathology is fundamental in understanding not only how the body is organized but also how the body works and how disease processes can affect it.

Likewise, preclinical animal research has been at the core of much of the progress made in medicine. Most, if not all, of what we know about the human body and biology, in general, has been initially made possible through animal research. A publication by the American Medical Association in 1989 listed medical advances emanating from animal research, including studies on AIDS, anesthesia, cardiovascular disease, diabetes, hepatitis, and Parkinson's disease, to name only a few [2]. More recently, in the field of transcatheter-delivered cardiac valves (see Chap. 36), the use of various animal models for preclinical research has been essential not only to optimize the device designs but also to ensure relative safety prior to their use in man. Furthermore, it has been through animal research that nearly all advances in veterinary medicine have also been established.

Animal research is still fundamental in developing new therapies aimed at improving the quality of life for patients with cardiovascular disease. Specifically, early cardiac device prototype testing is commonly performed utilizing animal models, both with and without cardiovascular disease. More specifically, before any invasively used device (a class III medical device) can be tested in humans, the Food and Drug Administration (FDA) requires that sufficient data be obtained from animal research indicating that the device functions in the desired and appropriate manner. It is also critical to subsequently extrapolate that a given device will be safe when used in humans, that is, it will behave in humans in a manner similar to its function in the chosen animal models in which it was tested. More specifically, this extrapolation of animal testing data to the human condition requires that the animal model(s) chosen for testing possesses similar anatomy and physiology as that of humans (normal and/or diseased). Unfortunately, detailed information relating human cardiac anatomy to that of the most common large mammalian animal models has been relatively lacking.

The following historical example illustrates how such a lack of knowledge can have a dramatic effect on the outcomes of cardiovascular research. During the 1970s and 1980s, dogs were employed as the primary animal model in numerous studies to identify potential pharmacological therapies for reducing infarct size. However, a detailed understanding of the coronary arterial anatomy was lacking or overlooked at the time; subsequently, it was shown that dogs have a much more extensive coronary collateral circulation relative to humans (Fig. 6.1). Thus, even when major coronary arteries were occluded, reliable and consistent

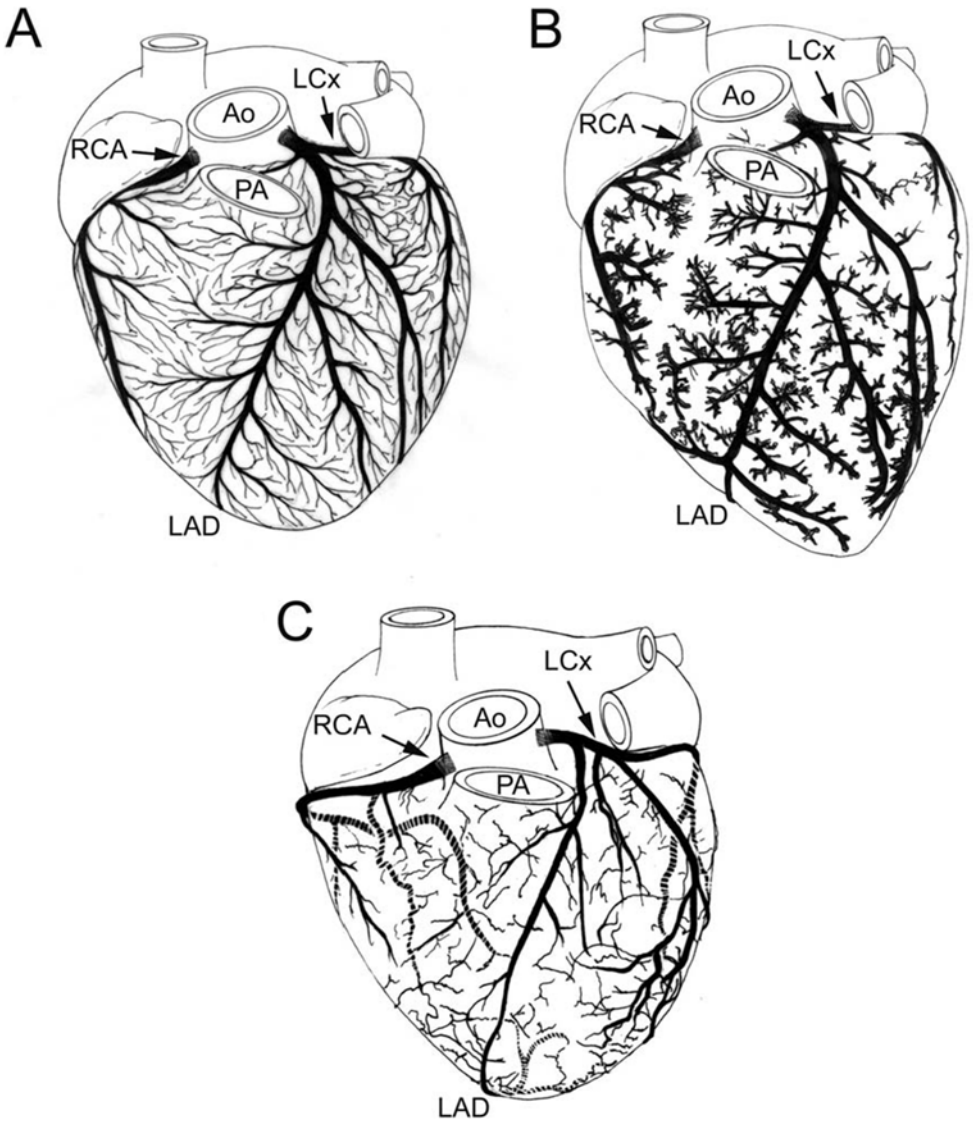

Fig. 6.1 Drawing of the coronary arterial circulation in the: (**A**) dog, (**B**) pig, and (**C**) human. Notice the extensive network of coronary collateralization in the dog heart, including many arterial anastomoses. The normal pig and human hearts have significantly less collateralization; each area of myocardium is usually supplied by a single coronary artery. *Ao* aorta, *LAD* left anterior descending artery, *LCx* left circumflex artery, *PA* pulmonary artery, *RCA* right coronary artery

myocardial infarcts were difficult to create. This led to false claims about the efficacy of many drugs in reducing infarct size which, when subsequently tested in humans, usually did not produce the same results as those observed in the canine experiments [5]. Therefore, ischemia studies with human-sized hearts have shifted to alternative species such as swine, which are considered to resemble the coronary collateral circulation of humans more precisely [6–9].

6.3 Literature Review of Large Mammalian Comparative Cardiac Anatomy

In general, the hearts of large mammals share many similarities, and yet the size, shape, and position of the hearts in the thoracic cavities can vary considerably between species [10]. Typically, the heart is located in the lower ventral part of the mediastinum in large mammals [11]. Most quadruped mammals tend to have a less pronounced left-sided orientation and a more ventrally tilted long axis of the heart when compared to humans [11] (Fig. 6.2). Additionally, hearts of most quadruped mammals tend to be elongated and have a pointed apex, with the exception of: (1) dogs which tend to have an ovoid heart with a blunt apex [11], (2) sheep which may have a somewhat blunt apex [12], and (3) pigs which have a blunt apex that is oriented medially [12]. Comparatively, human hearts typically have a trapezoidal shape [13] with a blunt apex. However, the apices of normal dog, pig, sheep, and human hearts are all formed entirely by the left ventricles [12–15] (Fig. 6.3).

It is important to note that differences exist in the heart weight to body weight ratios reported for large mammals. It is generally accepted that adult sheep and adult pigs have

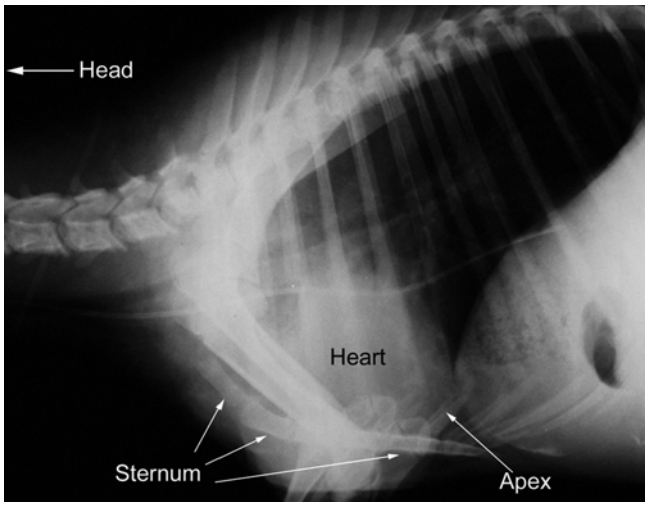

Fig. 6.2 Lateral radiograph of sheep thorax showing orientation of the heart while the animal is standing. The cranial direction is to the left and ventral to the bottom. The apex of the heart is more ventrally tilted (down toward the sternum) than is seen in humans, due to the posture of quadruped mammals. It should be noted, however, that this tilting is limited due to extensive attachments of the pericardium to the sternum and diaphragm

smaller heart weight to body weight ratios than those of adult dogs. More specifically, the adult dog may have as much as twice the heart weight to body weight ratio (6.9 to 7 g/kg) as pigs (2.9 to 2.5 g/kg) or sheep (3.0 to 3.1 g/kg) [16, 17], yet such findings will also likely be breed specific. The normal adult human heart weight to body weight ratio has been reported to be 5 g/kg which, on a comparative note, is similar to that of young pigs (25–30 kg animals) [7].

All large mammalian hearts are enclosed by the pericardium, which creates the pericardial cavity surrounding the heart. The pericardium is fixed to the great arteries at the base of the heart and is attached to the sternum and diaphragm in all mammals, although the degree of these attachments to the diaphragm varies between species [10, 11]. Specifically, the attachment to the central tendinous aponeurosis of the diaphragm is firm and broad in humans and pigs, the phrenopericardial ligament is the only pericardial attachment in dogs, and the caudal portion of the pericardium is attached via the strong sternopericardial ligament in sheep [10, 11].

The pericardium consists of three layers—the serous visceral pericardium (epicardium), the serous parietal pericar-

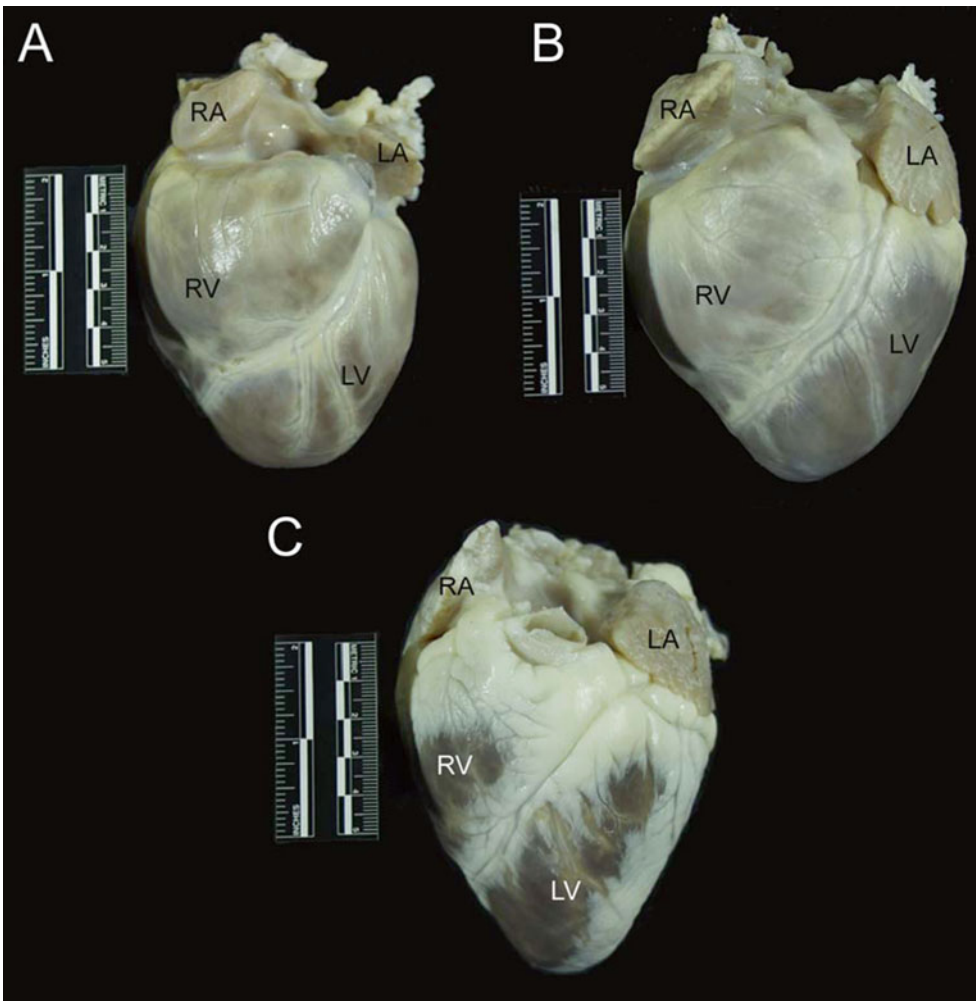

Fig. 6.3 The anterior aspect of the dog (**A**), pig (**B**), and sheep (**C**) hearts. The apex is formed entirely by the left ventricle in these hearts. Also notice the differences in overall morphology of the hearts. The dog heart is much more rounded than the pig and sheep hearts and has a blunt apex. The pig heart has more of a *valentine* shape with a somewhat blunt apex compared to the sheep heart. The sheep heart is much more conical in shape and has a much more pronounced apex than dog or pig hearts. Also noteworthy is the presence of significant amounts of epicardial fat on the sheep heart, compared with dog and pig hearts. *LA* left atrium, *LV* left ventricle, *RA* right atrium, *RV* right ventricle

dium, and the fibrous pericardium. The serous parietal pericardium lines the inner surface of the fibrous pericardium, and the serous visceral pericardium lines the outer surface of the heart. The pericardial cavity is found between the serous layers and contains the pericardial fluid. The pericardium is considered to serve many functions including: (1) preventing dilatation of the heart, (2) protecting the heart from infection and adhesion to surrounding tissues, (3) maintaining the heart in a fixed position in the thorax, and (4) regulating the interrelations between the stroke volumes of the two ventricles [18–20]. However, it should be noted that the pericardium is not essential for survival, since humans with congenital absence of the pericardium and pericardiectomized animals or humans can survive with minimal consequences for many years [18, 21].

Although the basic structure of the pericardium is the same, there are important differences between species [18, 19, 22]. For instance, pericardial wall thickness increases with increasing heart size [18]. Humans are the notable exception to this rule, having a much thicker pericardium than animals with similar heart sizes [18]. Specifically, the pericardium of the human heart varies in thickness between 1 and 3.5 mm [20], while the average thickness of the pericardium of various animal species was found to be considerably thinner (sheep hearts, 0.32 ± 0.01 mm; pig hearts, 0.20 ± 0.01 mm; dog hearts, 0.19 ± 0.01 mm) [19]. Differences in the amount of pericardial fluid are considered to exist as well. Holt reported that most dogs have 0.5–2.5 mL of pericardial fluid with some dogs having up to 15 mL, compared to 20–60 mL in adult human cadaver hearts [18]. For additional information on the pericardium, see Chap. 9.

The normally formed hearts of large mammals consist of four chambers—two thin-walled atria and two thicker walled ventricles. From both anatomical and functional perspectives, the heart is divided into separate right and left halves, with each half containing one atrium and one ventricle. In the fully developed heart with no associated pathologies, deoxygenated blood is contained in the right side of the heart and kept separate from oxygenated blood, which is on the left side of the heart. The normal path of blood flow is similar among all large mammals. Specifically, systemic deoxygenated blood returns to the right atrium via the caudal (inferior in humans) vena cava and the cranial (superior in humans) vena cava, subsequently passing into the right ventricle through the open tricuspid valve. At the same time, oxygenated blood returns from the lungs via the pulmonary veins to the left atrium and then through the open mitral valve to fill the left ventricle. After atrial contraction forces the last of the blood into the ventricles, ventricular contraction ejects blood through the major arteries arising from each ventricle, specifically the pulmonary trunk from the right ventricle and the aorta from the left ventricle. Via the pulmonary arteries, blood travels to the lungs to be oxygenated, whereas aortic blood travels through both the coronary arterial system (to feed the heart) and to the systemic circulation (to oxygenate bodily tissue). For additional discussions of flow patterns and function, see Chaps. 1 and 20.

6.3.1 The Atria

The right and left atria of the adult mammalian heart are separated by the interatrial septum. They are located at what is termed "the base" of the heart. The base receives all of the great vessels and is generally oriented cranially or superiorly, although there are reported differences in orientation among species, which are mostly dependent on the posture of the animal [13, 14, 23]. During fetal development, blood is able to pass directly from the right atrium to the left atrium, effectively bypassing the pulmonary circulation through a hole in the interatrial wall termed the *foramen ovale*. The foramen ovale has a valve-like flap located on the left atrial side of the interatrial septum, which prevents backflow into the right atrium during left atrial contraction [24]. At the time of birth or soon thereafter, the foramen ovale closes and is marked in the adult heart by a slight depression on the right atrial side of the interatrial wall termed the *fossa ovalis* [14, 24, 25]; it should be noted that it can remain patent in some individuals, and the rate of patent foramen ovale is comparable in adult humans and domestic swine at approximately 10–30 %. As compared to humans, the fossa ovalis is more posteriorly (caudally) positioned in dogs and sheep [11], but more deep-set and superior in the pig heart [13].

The sinus venosus, a common separate structure in non-mammalian hearts, is incorporated into the right atrium and is marked by the sinoatrial node in large mammals [24, 25]. According to Michaëlsson and Ho [11], all the mammals studied (including dogs, pigs, and sheep) have principally the same atrial architecture including: the sinus venosus, crista terminalis, fossa ovalis, Eustachian valve (valve of the inferior vena cava), and Thebesian valve (valve of the coronary sinus). All large mammalian atria also have an earlike flap called the auricle or appendage [13, 14, 25], although the size and shape of the auricles vary considerably between species [11, 13] (Fig. 6.4). In general, the junction between the right atrium and the right appendage is wide, whereas the junction on the left side is much more narrow [13]. Multiple pectinate muscles are found in both the right and left atrial appendages and on the lateral wall of the right atrium [11, 13, 14] (Figs. 6.5 and 6.6). Commonly, there is one posterior (caudal or inferior) and one anterior (cranial or superior) vena cava, although in some mammals there are two anterior venae cavae [24], and the location of the ostia of the venae cavae entering into the atrium varies [11, 13]. Specifically, the ostia of the inferior and superior vena cavae enter at right (or nearly right) angles in large mammalian animal models while entering the atrium nearly in line in humans [13].

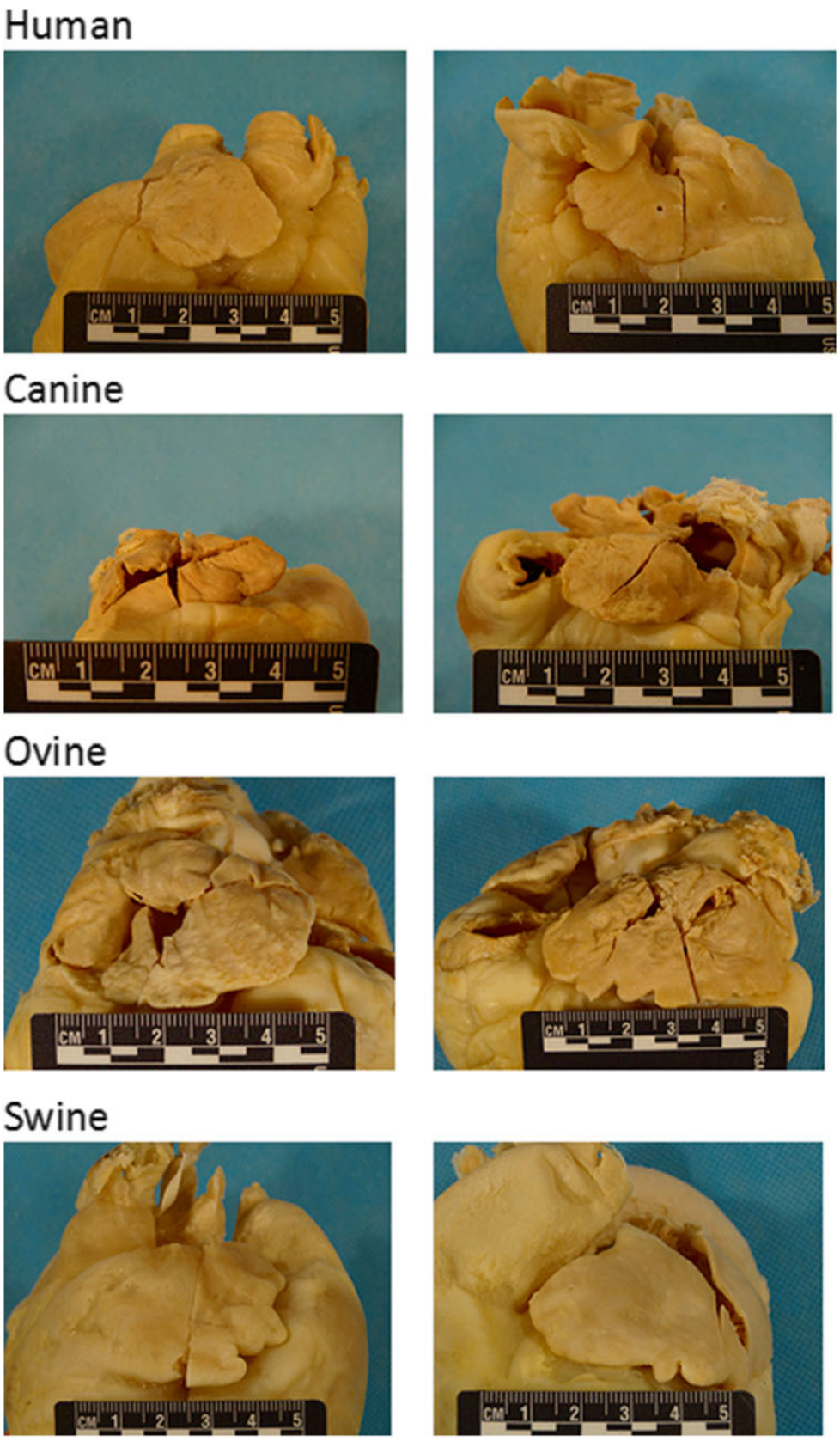

Fig. 6.4 Differences in large mammalian atria. Human: (*left*) Right atrial appendage is generally triangular in shape and may be larger or smaller than the left atrial appendage; (*right*) Left atrial appendage is generally tubular in shape. Canine: (*left*) Right atrial appendage is generally tubular and is larger than or similar in size to the left atrial appendage; (*right*) left atrial appendage is usually tubular. Ovine: (*left*) Right atrial appendage is generally half-moon in shape and is larger than the left atrial appendage; (*right*) left atrial appendage is generally triangular in shape. Swine: (*left*) Right atrial appendage is usually half-moon in shape and is generally smaller than the left atrial appendage; (*right*) left atrial appendage is generally triangular in shape. *Source*: www.vhlab.umn.edu/atlas, Comparative Anatomy Tutorial

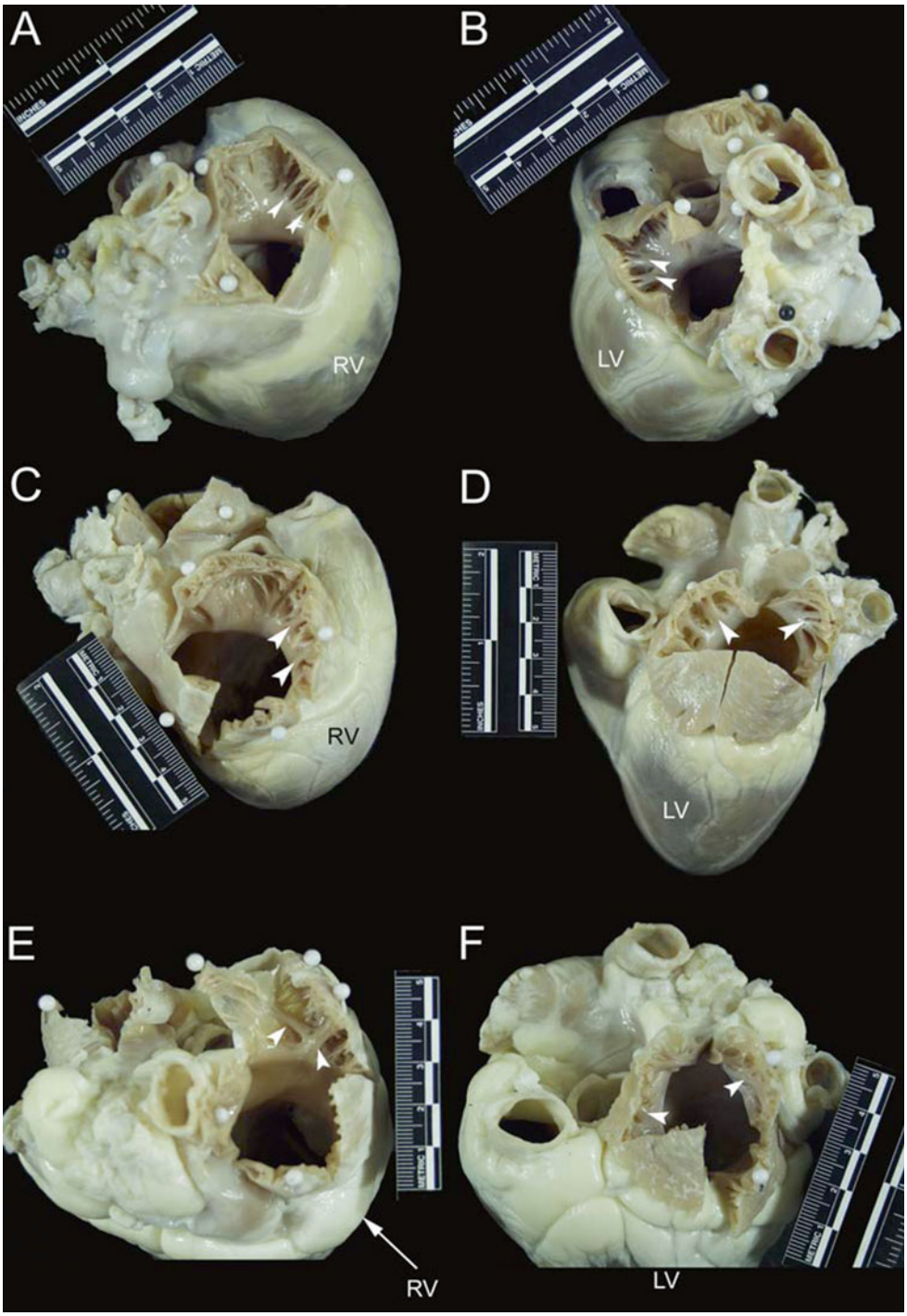

Fig. 6.5 The cranial (superior) aspect of dog (**A** and **B**), pig (**C** and **D**), and sheep (**E** and **F**) hearts. Images on the *left* of the figure (**A**, **C**, and **E**) show opened right atrial appendages, while images on the *right* (**B**, **D**, and **F**) show opened left atrial appendages. *White arrows* point to pectinate muscles that line the right and left atrial appendages. Notice that the *right* and *left* atrial appendages of the dog heart are tubular in nature. In contrast, the right and left atrial appendages of the pig and sheep heart are more triangular in morphology. *LV* left ventricle, *RV* right ventricle

Typically, the extent of the inferior vena cava between the heart and liver is long in domestic animals (>5 cm) and short in humans (1–3 cm) [11]. The coronary sinus ostium is normally located in the posterior wall of the right atrium, but its location can differ slightly between species. Interestingly, the number of pulmonary veins entering the left atrium also varies considerably between species; human hearts typically have four [13] or occasionally five [15], dog hearts have five or six [14], and pig hearts have two primary pulmonary veins [13]. In all large mammalian hearts, the atria are separated from the ventricles by a layer of fibrous tissue called the *cardiac skeleton*, which serves as an important support for the valves as well as to electrically isolate the atrial myocardium from the ventricular myocardium [23].

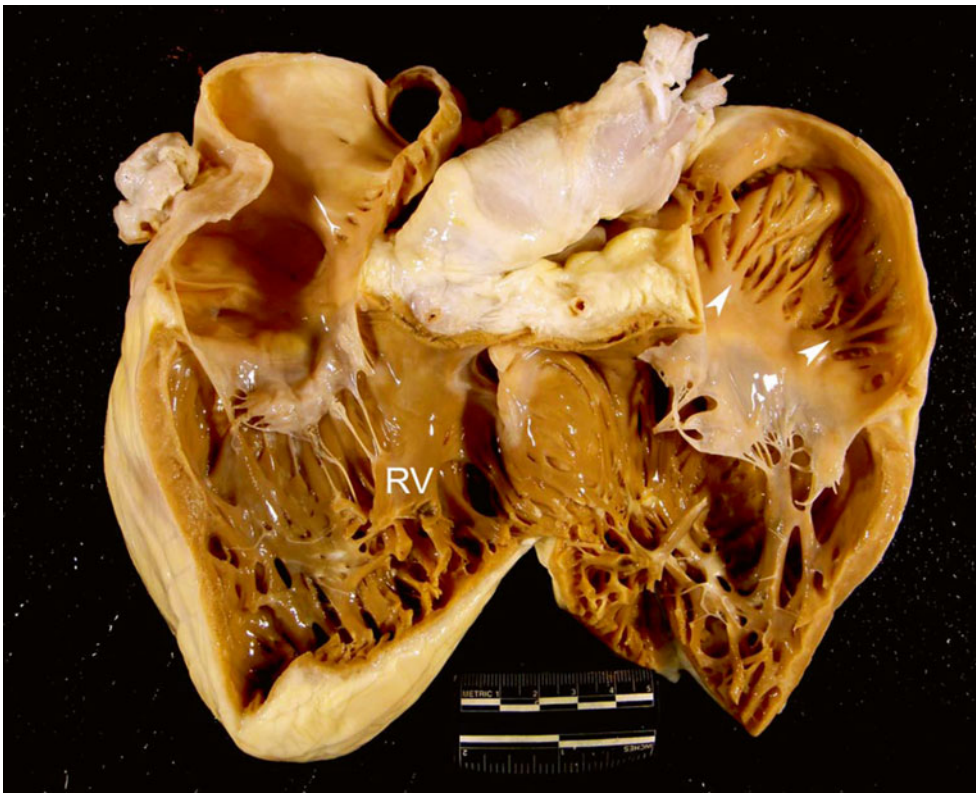

Fig. 6.6 A human heart opened on the inferior and superior aspects of the right ventricle, to show the anterior and posterior walls. *White arrows* point to pectinate muscles in the right atrial appendage on the anterior aspect. *RV* right ventricle

6.3.2 The Ventricles

The left and right ventricles of the large mammals used for cardiovascular research essentially contain the same components which are also structurally very similar to those in humans, including: an inlet (inflow) region, an apical region, and an outlet (outflow) region. The ventricles can be considered the major ejection/pumping chambers of the heart, and, as expected, their walls are significantly more muscular in nature than those of the atria. It should also be noted that the left ventricular walls are notably more muscular than those of the right ventricle, due to the fact that the left ventricle must generate enough pressure to overcome the resistance of the systemic circulation, which is much greater than the resistance of the pulmonary circulation (normally more than 4 times greater). The walls of both ventricles near the apex have interanastomosing muscular ridges and columns termed the *trabeculae carneae* which serve to strengthen the walls and increase the force exerted during contraction [11, 14, 24, 25]. However, large mammalian hearts reportedly do not have the same degree of trabeculation located in the ventricles as normal adult human hearts, and the trabeculations in animal hearts are commonly more coarse than those of human hearts [11, 13] (Figs. 6.7 and 6.8). One can also compare these relative anatomies by carefully studying various prepared plastinated cardiac specimens of large mammalian hearts, including humans. Papillary muscles supporting the atrioventricular valves are found attached to the walls of the ventricles. Similar to human anatomy, in the majority of large mammalian animal hearts, the right ventricle has three papillary muscles, and the left ventricle has two, although variations in individuals and species do occur [11]. It should be noted that, in general, each papillary muscle supplies chordae tendineae to at least 2 leaflets, ensuring redundancy. Both ventricles typically have cross-chamber fibrous or muscular bands, which usually contain Purkinje fibers. Within the right ventricle of most dogs, pigs, and ruminants, a prominent band termed the *moderator band* is typically present [11]. However, the origin and insertion of the band, as well as the composition of the band, differ notably between species. For example, in the pig heart, the band originates much higher on the septal wall compared to the analogous structure in the human heart [13], and the sheep heart has a similar moderator band as the pig heart (Figs. 6.6, 6.7, 6.8, and 6.9). In the dog heart, a branched or single muscular strand extends across the lumen from the septal wall near, or from the base of, the anterior papillary muscle [14] (Figs. 6.7, 6.8, 6.10, and 6.11). However, Truex and Warshaw [26] did not find any moderator bands in the dog hearts they examined ($n = 12$), but did observe them in all sheep hearts ($n = 12$) and all pig hearts ($n = 12$), compared to 56.8 % of the human hearts they examined ($n = 500$). Furthermore, they described three subtypes of moderator bands: a free arching band, a partially free arching band, and a completely adherent band.

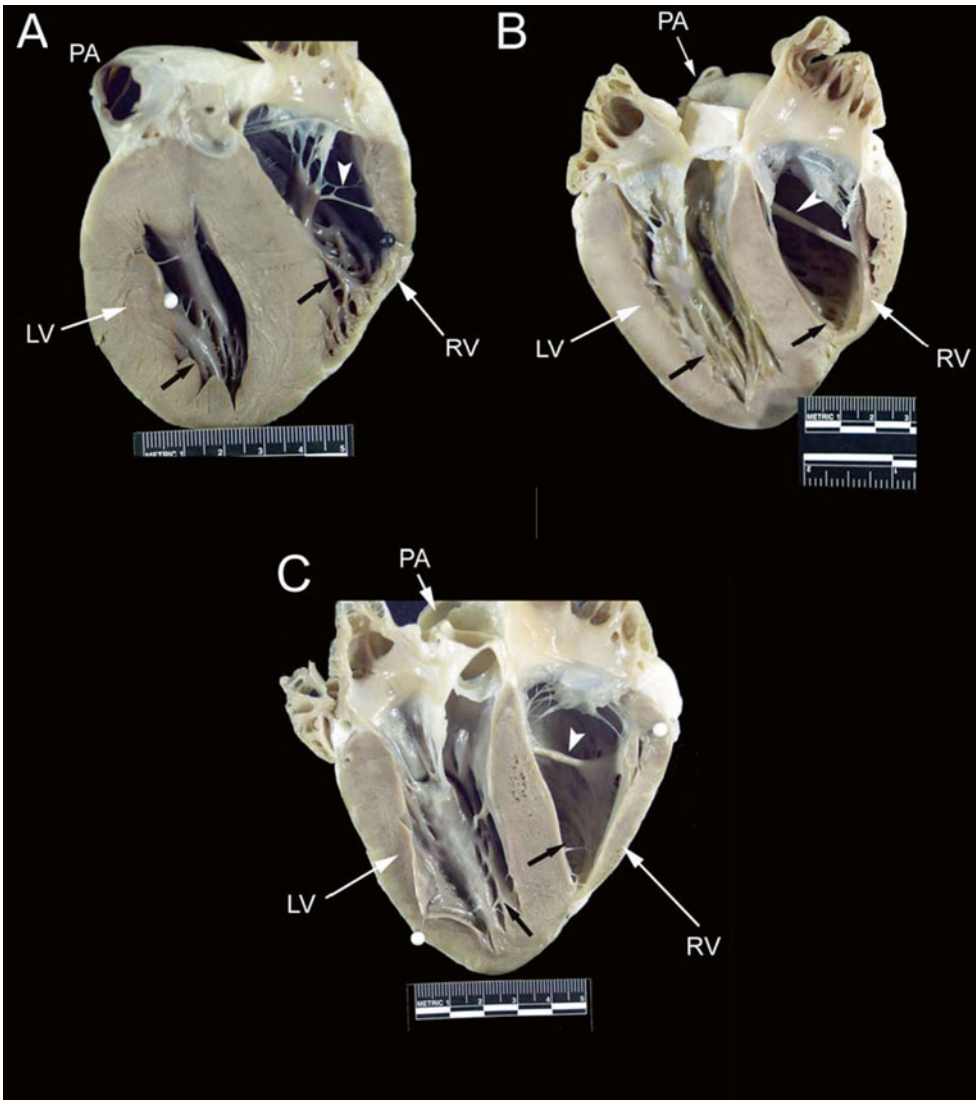

Fig. 6.7 Images showing dog (**A**), pig (**B**), and sheep (**C**) hearts that have been opened along the long axis to show both ventricular cavities. The anterior half of the heart is shown (left ventricle on the left and right ventricle on the right). *Black arrows* point to ventricular trabeculations which are large and coarse. *White arrows* point to the moderator band. Notice that a fibrous, branched moderator band extends from the anterior papillary muscle to the free wall in the canine heart. In contrast, a muscular, nonbranched moderator band extends from the septal wall to the anterior papillary muscle in pig and sheep hearts. Additionally, notice the presence of fibrous bands in the left ventricle. *LV* left ventricle, *PA* pulmonary artery, *RV* right ventricle

Nevertheless, one must also consider the potential for breed differences in animals and ethnic variability in humans. It is interesting to note that while, in general, anatomical textbooks state there is no specific structure named the moderator band in the left ventricle, left ventricular bands similar to the moderator band of the right ventricle have been described in the literature. For example, Gerlis et al. found left ventricular bands in 48 % of the hearts of children and in 52 % of the adult human hearts studied [27] (Fig. 6.8). They also reported that left ventricular bands were highly prevalent in sheep, dog, and pig hearts [27] (Fig. 6.7).

6.3.3 The Cardiac Valves

Large mammalian hearts have four cardiac valves with principally similar structures and locations. Two atrioventricular valves are located between each atrium and ventricle on both the right and left sides of the heart, and two semilunar valves lie between the ventricles and the major arteries arising from their outflow tracts (the pulmonary artery and aorta). Chordae tendineae connect the fibrous leaflets of both atrioventricular valves to the papillary muscles in each ventricle and serve to keep the valves from prolapsing into the atria during ventricular contraction, thereby preventing backflow of blood into the atria. The semilunar valves—the aortic and pulmonic—do not have attached chordae tendineae and close due to pressure gradients developed across them. See Chap. 34 for more details on valvular structures, function, and defects.

The valve separating the right atrium from the right ventricle is termed the *tricuspid valve* because it has three major cusps—the anterosuperior (anterior), inferior (posterior), and septal cusps. Typically, there are also three associated papillary muscles in the right ventricle. Interestingly, the commissures between the anterosuperior leaflet and the

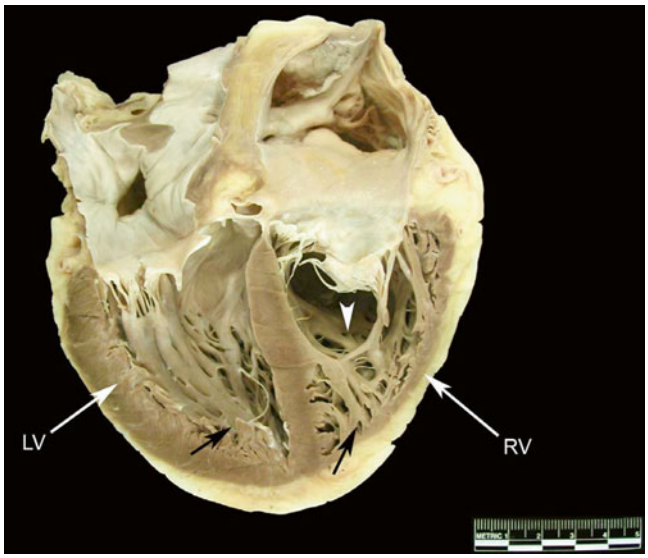

Fig. 6.8 Image of a human heart opened on the long axis to show both ventricular cavities. The left ventricle is on the left and the right ventricle on the right. *Black arrows* point to ventricular trabeculations, which are fine and numerous. The *white arrow* points to the moderator band, which is thick and muscular. It is different in size, shape, and location from the animal hearts shown in Fig. 6.7. *LV* left ventricle, *RV* right ventricle

inferior leaflets can be fused in dog hearts [14], giving the appearance of only two leaflets. Interindividual and interspecies variations in the number of papillary muscles have also been reported [11]. The valve separating the left atrium from the left ventricle is termed the *mitral or bicuspid valve* because it typically has two cusps, the anterior (aortic) and the posterior (mural). However, according to Netter [15], the human mitral valve actually can be considered to have four cusps, including the two major cusps listed above and two small commissural cusps or scallops; further publications on the mitral valve describe large variations in the number of scallops present in human hearts. Quill et al. studied the relative frequency of such variations in 38 human hearts and showed that the commonly described clefts on the posterior leaflet separating that leaflet into three regions (P1, P2, P3) were present in the majority of hearts; deviant clefts were also present in unexpected locations, such as the anterior leaflet, in some hearts [28]. In large mammalian hearts, two primary leaflets of the mitral valve are always present, but variations in the number of scallops exist and can be quite marked, giving the impression of extra leaflets [11]. A fibrous continuity between the mitral valve and the aortic valve is present in humans and most large mammals, extending from the central fibrous body to the left fibrous trigone [11] (Fig. 6.12). The length of this fibrous continuity, termed the *intervalvar septum or membranous septum*, varies considerably in length in different animals but notably is completely

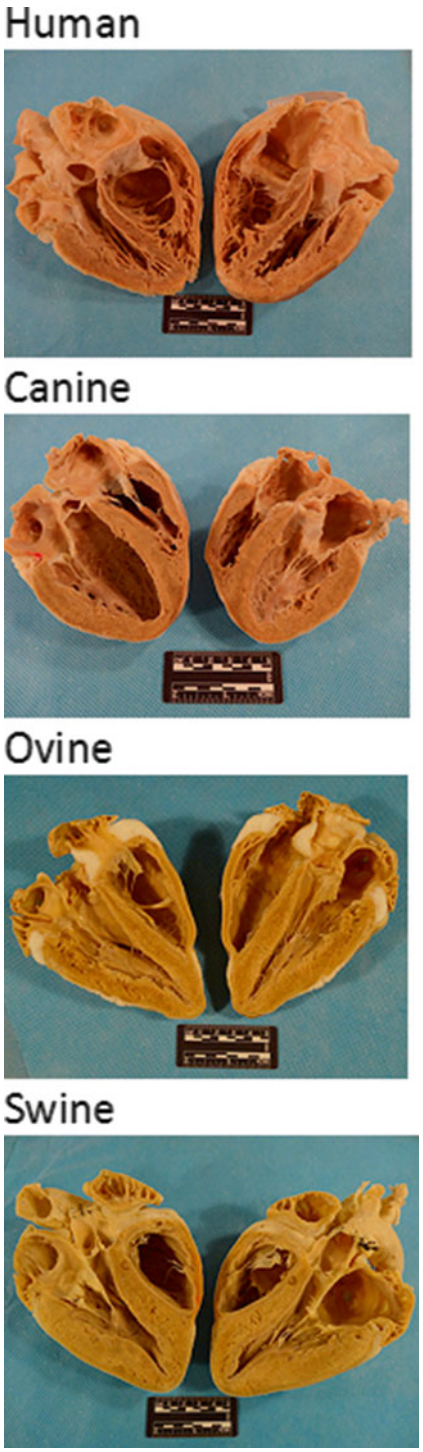

Fig. 6.9 Plastinated hearts of various species. *Human:* Trabeculae carneae in the apex are notably more numerous and finer than in the hearts of swine, canines, or sheep. *Canine:* Trabeculae carneae are coarser than those of humans; compared to swine and sheep hearts, the right ventricle has greater trabeculation though the left has similar trabeculation compared to these other animals. *Ovine:* Trabeculae carneae are noticeably fewer and coarser compared to those in human hearts. *Swine:* Trabeculae carneae are noticeably fewer and coarser compared to humans. *Source*: www.vhlab.umn.edu/atlas, Comparative Anatomy Tutorial

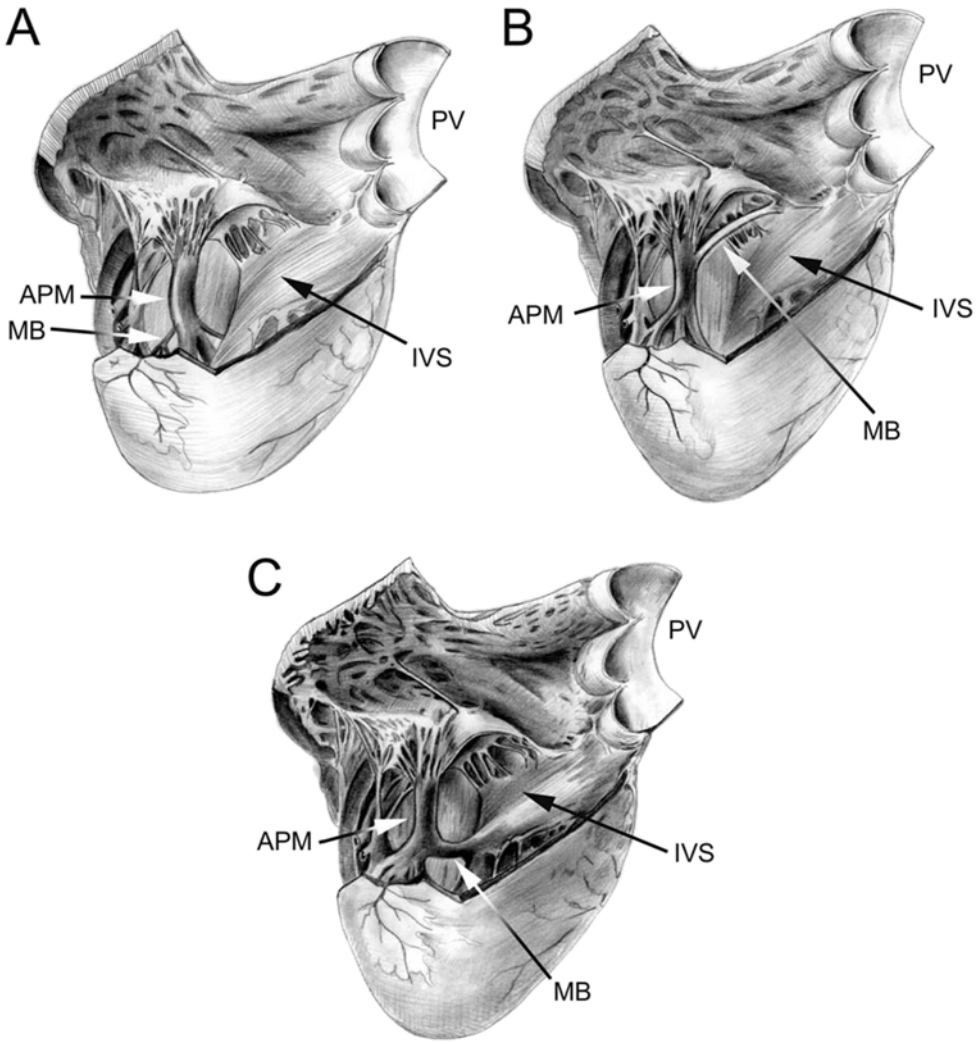

Fig. 6.10 Drawing of an opened right ventricular cavity in dog (**A**), pig and sheep (**B**), and human (**C**) hearts. The structure of the moderator band differs greatly between these hearts. In the dog heart, there is a branching fibrous band that runs from the anterior papillary muscle to the free wall of the right ventricle. In the human heart, the moderator band is typically located near the apex and is thick and muscular. In the pig and sheep hearts, the moderator band originates much higher on the interventricular septum and travels to the anterior papillary muscle. It is not as thick as in the human heart but is still muscular in nature. Also, note that the anterior papillary muscle in the dog heart originates on the septal wall, as opposed to originating on the free wall of the human, pig, and sheep hearts. *APM* anterior papillary muscle, *IVS* interventricular septum, *MB* moderator band, *PV* pulmonary valve

absent in sheep [29]. There are also differences in the fibrous ring supporting the mitral valve and in the composition of the leaflets of the mitral valve between species. For instance, according to Walmsley, a segment of the ring at the base of the mural cusp is always present in the human heart, but is difficult to distinguish in certain breeds of dogs and is inconspicuous in the sheep heart [29].

Differences in aortic valve anatomy have also been reported in the literature. For example, Sands et al. compared aortic valves of human, pig, calf, and sheep hearts [30], and they reported that interspecies differences in leaflet shape exist, but that all species examined had fairly evenly spaced commissures. Additionally, they found that variations in leaflet thickness existed; in particular, sheep aortic valves were described as especially thin and fragile. They also noted that there was a substantially greater amount of myocardial tissue supporting the right and left coronary leaflet bases in the animal hearts relative to humans [30].

6.3.4 The Coronary System

Mammalian hearts have an intrinsic circulatory system that originates with two main coronary arteries [11] whose ostia are located directly behind the aortic valve cusps. Deoxygenated coronary blood flow returns to the right atrium via the coronary sinus (into which the coronary veins drain) and also to the right atrium, the right and left ventricles [24, 31], and the left atrium [32, 33] by Thebesian veins. According to Michaëlsson and Ho [11], differences in perfusion areas exist between large mammalian species as well as within species (e.g., between breeds); these differences have also been described in humans. Dogs and sheep typically have a left coronary type of supply, such that the majority of the myocardium is supplied via branches arising from the left coronary artery. In contrast, pigs typically have a balanced supply where the myocardium is supplied equally from both right and left coronary arteries [11]. Yet, Crick et al. [13] reported that most of the pig hearts they examined

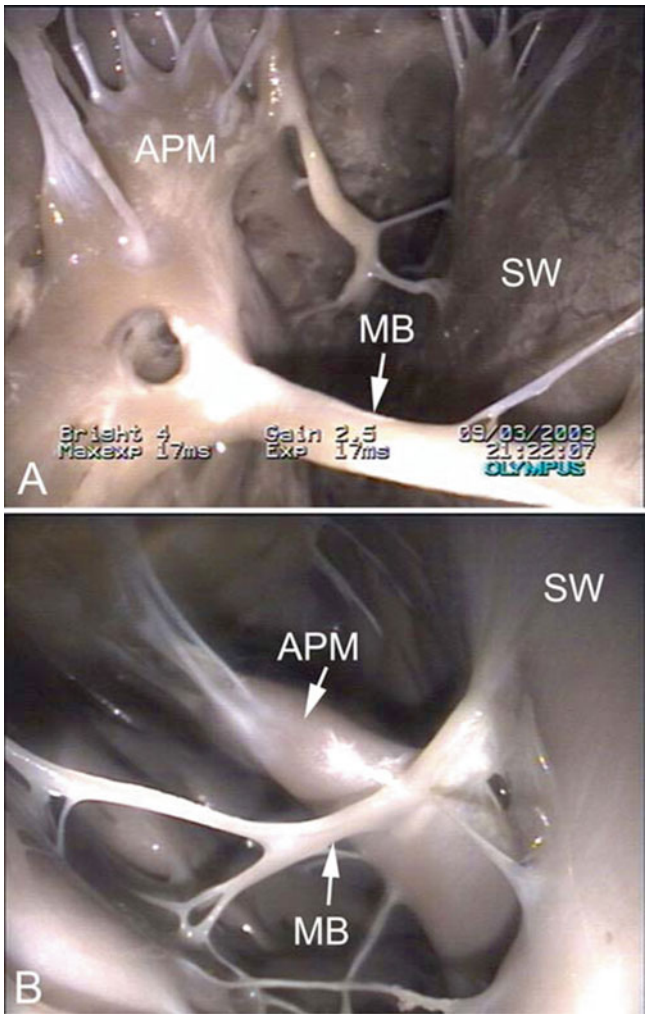

Fig. 6.11 Images showing the moderator band in the right ventricle of an ovine heart (**A**) and canine heart (**B**). The moderator band in the sheep is muscular, originating on the septal wall and running to the anterior papillary muscle. In contrast, the moderator band in the canine heart appears fibrous. It originates on the septal wall, runs to the anterior papillary muscle, and continues to the free wall of the right ventricle. *APM* anterior papillary muscle, *MB* moderator band, *SW* septal wall

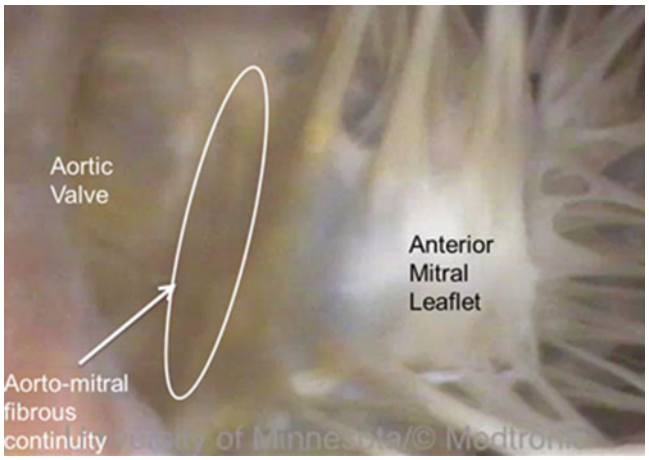

Fig. 6.12 Fibrous continuity between the mitral valve and aortic valve in a human heart. *Source*: www.vhlab.umn.edu/atlas, Left ventricle/Aortic valve/Visible Heart (functional)/Heart0284-2

(80 %) possessed right coronary dominance. Additionally, Weaver et al. [34] found that the right coronary artery was dominant in 78 % of the pigs they studied. Most human hearts (approximately 90 %) also display right coronary arterial dominance [35].

Another important aspect of the coronary arterial circulation, one that is of great importance in myocardial ischemia research, is the presence or absence of significant collateralization of the coronary circulation. Normal human hearts tend to have sparse coronary collateral development, which is very similar to that seen in normal pig hearts [34]. In contrast, it is now widely known that extensive coronary collateral networks can be seen in normal dog hearts [5, 36–39]. Furthermore, Schaper et al. [40] found that the coronary collateral network of dogs was almost exclusively located at the epicardial surface, while that of pig hearts, when present, was located subendocardially. They were unable to detect a significant collateral network in the hearts of sheep (Fig. 6.1).

There are three major venous pathways that drain the heart—the coronary sinus, anterior cardiac veins, and Thebesian veins [33, 41]. Drainage from each of these venous systems is present in human hearts as well as in dog, pig, and sheep hearts [13, 14, 24, 33]. While the overall structure of the coronary venous system is similar across species, interindividual variations are common. Nevertheless, there is one notable difference in the coronary venous system between species that warrants mention, that is, the presence of the left azygos vein draining the left thoracic cavity directly into the coronary sinus; a left azygos vein is typically present in both pig [13] and sheep [11] hearts (Fig. 6.13).

6.3.5 The Lymphatic System

In addition to an intrinsic circulatory system, large mammalian hearts have an inherent and substantial lymphatic system which serves the same general function of the lymphatic system in the rest of the body. More specifically, the mammalian lymphatic system has been described as follows. Hearts have subepicardial lymphatic capillaries that form continuous plexuses covering the whole of each ventricle [42]. Furthermore, the lymphatic channels are divided into five orders, with the first order draining the capillaries and joining to become the second order and so on, until the lymph is drained from the heart via one large collecting duct of the fifth order. In general, it has been described that dogs, pigs, and humans have extensive subepicardial and subendocardial networks with collecting channels directed toward large ducts in the atrioventricular sulcus that are continuous with

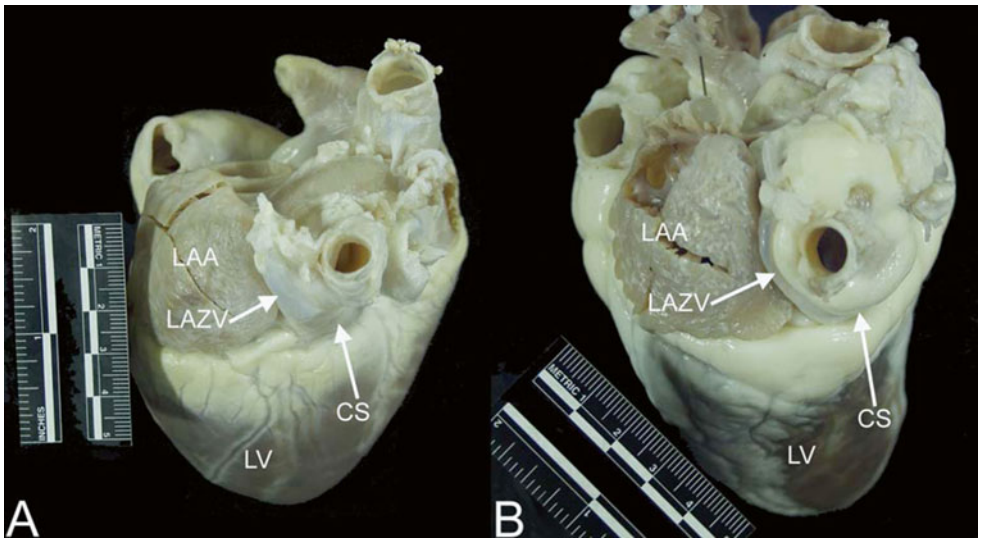

Fig. 6.13 Images showing the left azygos (hemiazygos) vein entering the coronary sinus in the pig (**A**) and sheep (**B**) hearts. The left azygos vein drains the thoracic cavity directly into the coronary sinus in these animals, rather than emptying into the superior vena cava via the azygos as seen in dog and human hearts. Notice that it travels between the left atrial appendage and the pulmonary veins; the oblique vein of Marshall (oblique vein of the left atrium) travels this path in human and dog hearts. *CS* coronary sinus, *LAA* left atrial appendage, *LAZV* left azygos vein, *LV* left ventricle

the main cardiac lymph duct [43]. Furthermore, it was found that the lymphatic vessels of the normal heart are distributed in the same manner as the coronary arteries and follow them as two main trunks to the base of the heart [44].

6.3.6 The Conduction System

All large mammalian hearts have a very similar conduction system whose main components are the sinoatrial node, atrioventricular node, bundle of His, right and left main bundle branches, and Purkinje fibers. Yet, interspecies variations are well recognized, especially with regard to the finer details of the arrangement of the transitional and compact components of the atrioventricular node [11]. In the mammalian heart, the sinoatrial node is the normal pacemaker [11, 24, 25] and is situated in roughly the same location in all hearts: high on the right atrial wall near the junction of the superior vena cava and the right atrium. Conduction spreads through the atria to the atrioventricular node (which interestingly is unique to both birds and mammals) [25] and then to the bundle of His, which is the normal conducting pathway from the atria to the ventricles, penetrating through the central fibrous body. The right and left main bundle branches emanate from the bundle of His and branch further into the Purkinje fibers which then rapidly spread conduction to the ventricles [11]. The atrioventricular node and bundle of His are typically located subendocardially in the right atrium within a region known as the *triangle of Koch*, which is delineated by the coronary sinus ostium, the membranous septum, and the septal/posterior commissure of the tricuspid valve (Fig. 6.14). The presence of the *os cordis* has been noted to be present in the sheep heart, but not in dog, pig, or human hearts. Specifically, it is a small, fully formed bone that lies deep in the atrial septum which, in turn, influences the location and course of the bundle of His in sheep hearts. Other known differences in the atrioventricular conduction system between human, pig, dog, and sheep hearts are illustrated in Table 6.1. For more details on the conduction system, see Chap. 13.

6.4 Qualitative and Quantitative Comparisons of Cardiac Anatomy in Commonly Used Large Mammalian Cardiovascular Research Models

The following section describes original research conducted at the University of Minnesota by the authors of this chapter.

6.4.1 Importance for Comparing the Anatomy of Various Animal Models

Selection of the proper experimental model for use in cardiovascular research depends on many factors including: (1) cost, (2) quality and quantity of data, (3) familiarity with the model, and/or (4) relevance to the human condition [49]. Typically, a balance as to the relative importance of these factors is determined when optimizing any experimental protocol. Yet, one important parameter that is often overlooked in such a design is the comparative cardiac anatomy of the model in question relative to that of humans.

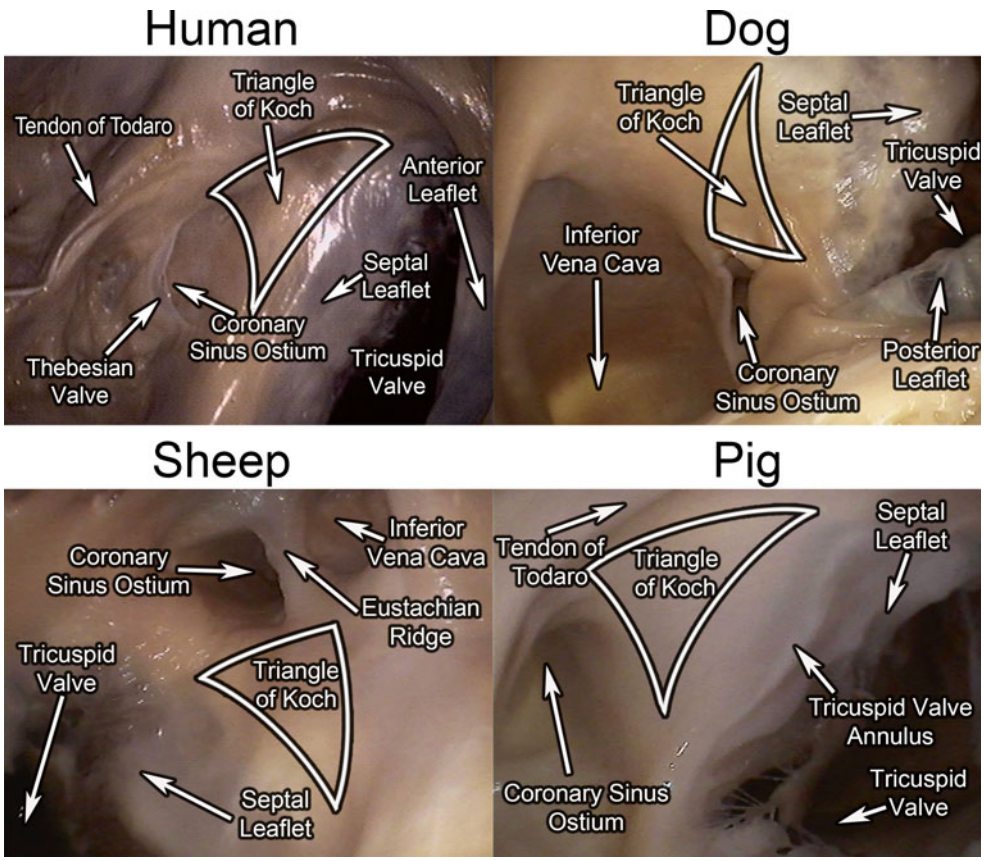

Fig. 6.14 The *triangle of Koch* in human, dog, sheep, and pig hearts

Even today, there is often considerable debate over which cardiovascular research model most closely resembles the human heart anatomically. Surprisingly, in spite of this debate, the comparative cardiac anatomy of such models as a specific topic is largely unexplored. Nevertheless, this question is especially important for biomedical device design and testing in which the goal is to test a product that directly interacts with specific anatomical structures. Furthermore, such comparisons often become even more complicated due to: (1) the relative orientation and/or position of each species' heart and (2) the various terminologies used to describe heart anatomy and position (attitudinally correct anatomy) which can vary between various animal models and in comparison to humans. In addition, one hopes to match the cardiac dimensions across species, but this can be further complicated by both gender and age. For example, a 6–7-month-old Yorkshire swine has a typical cardiac mass between 300 and 400 g, which is similar to that of the healthy adult human. Finally, genetic heritage influences expressed cardiac anatomy, and specific descriptors are often missing in previous reports (i.e., specific breeds of animals studied).

Thus, the following studies were designed to elucidate the major similarities and differences between the hearts of several major large mammalian cardiovascular research models and then relate these findings to humans. Specifically, qualitative and quantitative techniques were employed on post-mortem, formalin-fixed porcine, ovine, canine, and human hearts.

6.4.2 Methods and Materials

For this study, we obtained fresh hearts of humans (*Homo sapiens*; man), pigs (*Sus domestica*; swine, porcine), dogs (*Canis lupus familiaris*; canine), and sheep (*Ovis aries*; ovine). Human hearts ($n=8$) were obtained from the Anatomy Bequest Program at the University of Minnesota. All human hearts were previously unfixed and devoid of clinically diagnosed heart disease or defect. Swine (Yorkshire cross), canine (hound cross), and ovine (Polypay cross) ($n=10$ each) hearts were obtained from either Research Animal Resources at the University of Minnesota or the Physiological Research Laboratories at Medtronic, Inc. These animals were used for prior research studies that did not alter their anatomy. In other words, in all cases, care was taken to insure that hearts were only obtained from individuals and animals in which cardiac anatomy was not considered to be altered by disease processes or any prior experimental protocols.

6.4.2.1 Heart Preservation

To preserve the hearts and prepare them for comparative anatomical study, specimens were all similarly *pressure*

Table 6.1 Similarities and differences in the atrioventricular conduction systems of dog, pig, sheep, and human hearts [45–48]

	Location of AV node	AV node and bundle of His junction	Length of bundle of His	Route of bundle of His
Human	Located at the base of the atrial septum, anterior to the coronary sinus, and just above the tricuspid valve	End of the AV node and the beginning of bundle of His are nearly impossible to distinguish	Total length of the unbranched portion is 2–3 mm. Penetrating bundle is 0.25–0.75 mm in length. Bundle bifurcates just after emerging from the central fibrous body	Bundle lies just beneath the membranous septum at the crest of the interventricular septum
Pig	Lies on the right side of the crest of the ventricular septum and is lower on the septum than in humans	No explicit information found	Penetrating bundle is very short in comparison to humans	Climbs to the right side of the summit of the ventricular septum, where it enters the central fibrous body. The bifurcation occurs more proximally than in humans
Dog	Same as in humans	Consists of internodal tracts of myocardial fibers	Penetrating bundle is 1–1.5 mm long, significantly longer than the human penetrating bundle	His bundle runs forward and downward through the fibrous base of the heart, just beneath the endocardium. There are at least three discrete bundle of His branches of myocardium that join the atrial end of the AV node via a proximal His bundle branch
Sheep	Located at the base of the atrial septum, anterior to the coronary sinus, just above the tricuspid valve, and at the junction of the middle and posterior one-third of the os cordis	Junction is characterized by fingerlike projections, where the two types of tissue overlap; size and staining qualities of the initial Purkinje cells of the bundle of His make it easy to distinguish between the end of the AV node and the beginning of the bundle of His	Portion of the bundle passing through the central fibrous body is ~1 mm. Bundle extends 4–6 mm beyond the central fibrous body before it bifurcates	Unbranched bundle must pass beneath the os cordis to reach the right side of the ventricular septum. The bundle of His then remains relatively deep within the confines of the ventricular myocardium. Branching occurs more anteriorly in sheep than in humans

AV atrioventricular

perfusion fixed. Briefly, this consisted of suspending each heart in a large container of 10 % buffered formalin from cannulae tied into the following major vessels: the superior caval vein, the pulmonary trunk, the aorta, and one pulmonary vein. All remaining vessels were sealed, with the exception of small vents positioned in both the inferior caval vein and in one of the pulmonary veins. Formalin was gravity fed down the cannulae from a reservoir chamber positioned 35–40 cm above the fluid level in the suspension chamber. This system generated a reproducible perfusion pressure between 45 and 50 mmHg. The hearts were allowed to fix under these conditions for a minimum of 24 h in order to allow for adequate penetration of fixative. This method of fixation was quite reproducible to ensure that the hearts maintained a similar anatomical configuration.

6.4.2.2 Qualitative Anatomical Assessment of Perfusion-Fixed Hearts

Several observational assessments, similar to those conducted and previously described by Crick et al. [13], were completed on each heart. In addition to these assessments, a 6 mm endoscopic camera (Olympus Optical, Tokyo, Japan) was inserted into each chamber of each heart, with care taken not to distort any structure to be observed. This allowed for direct visualization of the internal chambers of the heart without dissection, hence allowing the anatomical structures to be examined in a more realistic state. Specific anatomical features assessed included:

- Overall shape of entire heart (conical, valentine, trapezoidal, elliptical, or rounded with blunt apex; Fig. 6.3)
- Overall shape and size of atria and free portions of the appendages (triangular, half-moon, or tubular)
- Ventricular formation of the apex (right, left, or both ventricles)
- Number of pulmonary veins (best estimates were made as some pulmonary veins were dissected close to the atrium)
- Presence or absence of noncardiac coronary sinus tributaries (left azygos vein)
- General shape of:
  - Inferior caval vein ostium
  - Superior caval vein ostium
  - Pulmonic valve

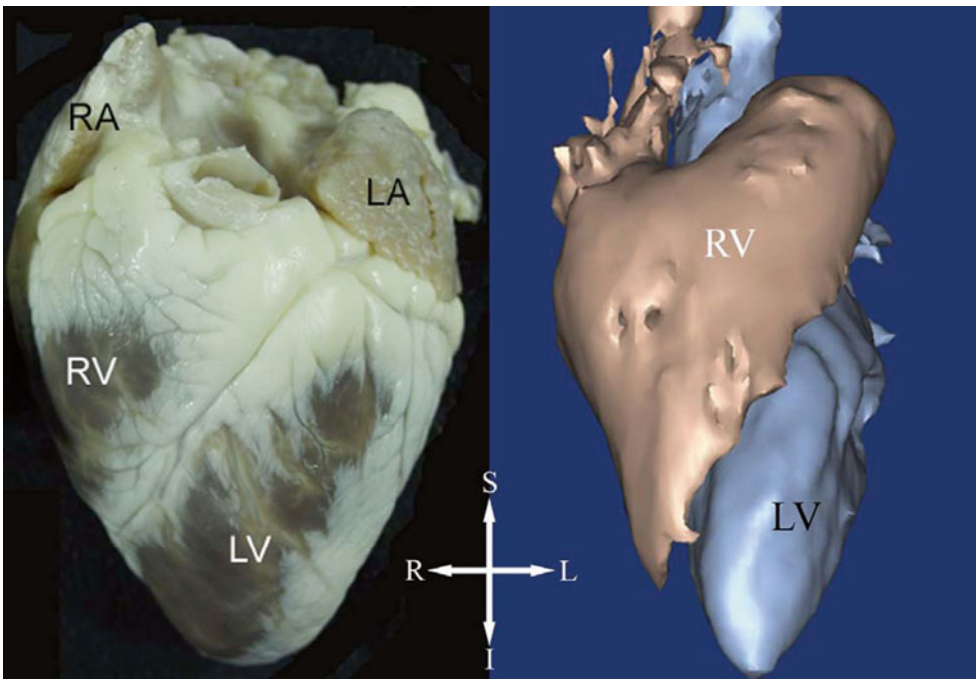

Fig. 6.15 Anterior surface of a fixed sheep heart and end-diastolic volumetric reconstruction of a sheep heart from magnetic resonance images. Note that the apex of the sheep heart is pointed inferiorly and slightly anteriorly. *LA* left atrium, *LV* left ventricle, *RA* right atrium, *RV* right ventricle

  - Tricuspid valve
  - Aortic valve
  - Mitral valve
  - Coronary sinus ostium
- Presence or absence of the valve of the coronary sinus ostium (Thebesian valve)
- Presence or absence of the moderator bands of the right ventricles (if present, the locations of attachment points were noted)
- Number of papillary muscles found in the right and left ventricles
- Degree of trabeculation of right and left ventricular endocardium (1–5; 1 = no trabeculations, 5 = highly trabeculated)
- Presence or absence of any left ventricular bands (i.e., similar structures to the moderator bands of the right ventricle).

6.4.2.3 Quantitative Anatomical Assessments of Perfusion-Fixed Hearts

The following quantitative measurements were performed on each heart by employing a novel 3D technique. Briefly, a MicroScribe® 3D digitizing arm (3DX, Immersion Corp., San Jose, CA, USA), consisting of a touch probe with six degrees of freedom, was used to gather the 3D data points. First, each heart was suspended and stabilized within a rectangular metal frame via sutures placed into the aorta, the right and left lateral ventricular walls, and the apex. More specifically, the heart was suspended in the classic *valentine heart* position, with the apex pointing toward the bottom of the frame and base toward the top, for easy comparison between hearts. In all cases, attitudinally correct nomenclature was used to describe structures in a more meaningful manner (Figs. 6.15 and 6.16; see also Chap. 2). To allow for the generation of a consistent coordinate axis system, three small holes for touch probe placement were drilled into a right angle scribe that was affixed to a corner of the support structure. This setup allowed for a consistent reference frame for all subsequent digitizations; each heart was maintained within the same 3D space, allowing for precise measurement between all digitized locations. Furthermore, this overall setup and experimental design allowed for free movement of the 3DX probe as the reference frame could be regenerated following each movement, allowing for complete probe access to all desired aspects of the heart.

For probe initialization, the coordinate axes were set up using the acquisition software (Inscribe, Immersion Corp.) on the right angle scribe by digitizing the location of the three holes that were set up as the origin, a point on the *x*-axis, and a point on the *y*-axis; the software then automatically generated the *z*-axis. Prior to dissection, eight external locations were digitized in each heart (Table 6.2) such that comparisons of the major external dimensions could be performed (Table 6.3). Then, small incisions were made in the right and left atrial appendages to allow for internal access in each heart. With the simultaneous use of endoscopic cameras, the touch probe was navigated to specific locations in each heart such that comparisons of valve dimension, ventricular chamber dimension, and those of the coronary sinus ostium could be subsequently calculated (Tables 6.2 and 6.3). It should be noted that all orientational terms are in rela-

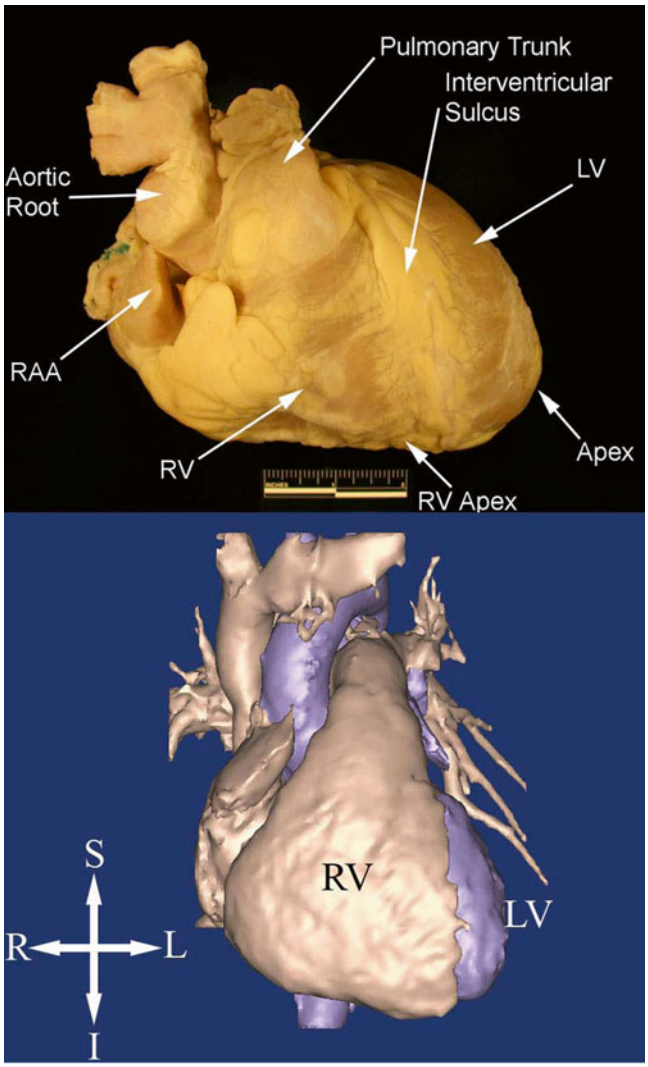

Fig. 6.16 Anterior surface of a fixed human heart and end-diastolic volumetric reconstruction of a human heart from magnetic resonance images. Note that the apex of the human heart is pointed to the left and slightly anteriorly. *LV* left ventricle, *RAA* free portion of right atrial appendage, *RV* right ventricle

tion to the reference frame, which closely mimics the orientation of the animal hearts in vivo. However, these terms do not necessarily describe the exact positions of the human hearts in vivo. In total, only three measurements from porcine heart number 1 needed to be removed due to improper coordinate axis regeneration. These were (1) posterior base to whole heart apex, (2) aortic valve mid-left coronary cusp to left ventricular apex, and (3) aortic valve center to left ventricular apex.

All calculations were analyzed both as raw data and as normalized data (divided by the given heart weight). Statistical significance tests were performed using one-way ANOVA and Bonferroni post analyses; significance was set at $\alpha = 0.05$. All values are presented as means ± standard deviation.

6.4.3 Results

The average heart weights were 367.3 ± 65.8 g for humans, 274.6 ± 50.4 g for pigs, 258.1 ± 36.2 g for dogs, and 353.1 ± 120.7 g for sheep. Human heart weights were significantly larger than dog heart weights ($p < 0.05$). The average age of the human donors was 63.8 ± 19.5 years. Although the exact age of the animals was not known, all porcine hearts were from younger rapidly growing animals (<1 years old); all canine (1–2 years old) and ovine hearts (1–3 years old) were from mature animals. Six of the human hearts were obtained from females and 2 were from males. All porcine and canine hearts were from male animals, while all ovine hearts were from female animals.

6.4.3.1 Qualitative Comparisons

The human hearts had the largest variation in overall shape compared to the animal hearts. Three human hearts were classified as having an elliptical shape, 2 were conical, 2 were rounded with a blunt apex, and 1 was valentine shaped. The overall defined shapes of the animal hearts were as follows: 6 ovine hearts were considered conical and 4 were valentine; 8 porcine hearts were valentine and 2 were trapezoidal; and all 10 canine hearts were elliptical. Nevertheless, the apexes of the hearts were formed entirely by the left ventricles in all animal hearts and in 5 of the 8 human hearts. In the other 3 human hearts, the apexes were mostly left but were considered slightly shifted toward a "joint apex."

Generally, the free portions of the right atrial appendages of the human hearts were defined as either triangular (7 of 8) or tubular on the left (8 of 8). The size of the free portion of the appendages was variable in the human hearts with 3 having larger right appendages, 3 having larger left appendages, and 2 having similar sized appendages. The free portions of the right atrial appendages of the ovine hearts were in the shape of a half-moon (9 of 10) and typically characterized as triangular on the left (8 of 10). The free portions of the right atrial appendages were larger than the left in 7 hearts and the same size as the left in the remaining 3 hearts. The free portions of the right atrial appendages of the porcine hearts were generally in the shape of a half-moon (9 of 10) and typically triangular on the left (6 of 10). The left atrial appendage was larger than the right in 9 hearts and the same size in the remaining heart. In the canine hearts, the free portions of both atrial appendages were considered to be tubular in 9 hearts and triangular in 1 heart. The free portions of the right atrial appendages were larger than the left in 5 hearts and the same

Table 6.2 Digitized locations

External locations	*Description*
Base	Anterior (anterosuperior) at the origin of the pulmonary trunk Posterior (posteroinferior) at the junction of the coronary sulcus and the interventricular sulcus Right lateral at the right atrial/right ventricular junction Left lateral at the left atrial/left ventricular junction
Apex coronary sinus	At the true apex of the heart (LV) The entry of the coronary sinus into the right atrium on the posterior aspect of the heart and three evenly spaced points to the end of the coronary sinus, defined as the junction of the great cardiac vein and the oblique vein of the left atrium (Marshall)
Internal locations	*Description*
Tricuspid valve	Anterior (superior) Posterior (inferior) Septal (posterior) Lateral (anterior) Center—best approximation
Coronary sinus	Superior (posterolateral) Inferior (anteroseptal) Lateral (superior) Septal (inferior) Thebesian valve leading edge (when present) Center—best approximation
Pulmonic valve	Midpoint on anterior cusp Midpoint of right cusp Midpoint of left cusp Center—best approximation
RV apex mitral valve	Deepest point in the RV apex Anterior (superior) Posterior (inferior) Septal (posterior) Lateral (anterior) Center—best approximation
Aortic valve	Midpoint of right coronary cusp Midpoint of left coronary cusp Midpoint of non-coronary cusp Right coronary/left coronary commissure tip Right coronary/non-coronary commissure tip Left coronary/non-coronary commissure tip Center—best approximation
LV apex	Deepest point in the LV apex

size as the left in the other 5 hearts. The left azygos (hemiazygos) vein was present as a tributary to the coronary sinus in all ovine and porcine hearts examined; it was not present in any of the canine hearts or human hearts. Thebesian valves covering some aspect of the coronary sinus ostium were present in all human hearts, but absent in all animal hearts examined.

Moderator bands were present in the right ventricles of all hearts examined (Figs. 6.7, 6.8, 6.10, and 6.11). However, the origin and attachment of these bands, as well as their appearance, were varied among species. In the human hearts, the moderator band typically arose more apically on the septal wall and attached to the base of the anterior papillary muscle (APM). Interestingly, the band was a free arc in 6 of the hearts and a ridge in 2 hearts. In both sheep and pigs, the moderator bands presented as muscular structures that originated on or near the septal papillary muscle (SPM), inserted at the body or head of the APM, and were free arcs in all. In contrast, the moderator bands of the canine hearts presented as fibrous networks that originated on the APM or septal wall and inserted on the free walls of the right ventricles (usually at multiple sites). Similar to all pig and sheep hearts and 75 % of the human hearts, the canine moderator band was a free arching structure across the ventricular cavity. There were left ventricular bands, similar to the moderator band (composed of or containing what are considered to be conduction fibers), identified in all but 1 porcine heart and 1 human heart.

All human, ovine, and porcine hearts had one well-defined APM in the right ventricle. In contrast, 6 canine hearts had 2 APMs and 4 hearts had a single APM. Nine ovine hearts had a single posterior papillary muscle (PPM) in the right ventricle and 1 heart had 2 PPMs. Six porcine hearts had a single PPM, 3 hearts had 2 PPMs, and 1 heart had 3 PPMs. Only 1 canine heart had a single PPM, 5 hearts had 2 PPMs, and 4 hearts had 3 PPMs. Three human hearts had a single PPM, 1

Table 6.3 Calculated measurements

External measurements	*Description*
Base to apex length	Anterior (anterosuperior) to apex Posterior (posteroinferior) to apex Right lateral to apex Left lateral to apex
Coronary sinus	Length of the coronary sinus
Internal measurements	*Description*
Coronary sinus ostium	Superior (posterolateral) to inferior (anteroseptal) diameter Lateral (inferior) to septal (superior) diameter Functional ostium—Thebesian valve to septal (superior) diameter
Tricuspid valve	Anterior (superior) to posterior (inferior) diameter Septal (posterior) to lateral (anterior) diameter
Right ventricular inflow	Anterior (superior) tricuspid valve to apex distance Posterior (inferior) tricuspid valve to apex distance Septal (posterior) tricuspid valve to apex distance Lateral (anterior) tricuspid valve to apex distance Center tricuspid valve to apex distance
Pulmonic valve	Sinotubular junction diameter Basal annular diameter
Right ventricular outflow	Mid-anterior cusp pulmonic valve to apex distance Mid-right cusp pulmonic valve to apex distance Mid-left cusp pulmonic valve to apex distance Center pulmonic valve to apex distance
Mitral valve	Anterior (superior) to posterior (inferior) diameter Septal (posterior) to lateral (anterior) diameter
Left ventricular inflow	Anterior (superior) mitral valve to apex distance Posterior (inferior) mitral valve to apex distance Septal (posterior) mitral valve to apex distance Lateral (anterior) mitral valve to apex distance Center mitral valve to apex distance
Aortic valve	Sinotubular junction diameter Basal annular diameter
Left ventricular outflow	Mid-right coronary cusp aortic valve to apex distance Mid-left coronary cusp aortic valve to apex distance Mid-non-coronary cusp aortic valve to apex distance Center aortic valve to apex distance

heart had 2 PPMs, and 4 hearts had 3 PPMs. Eight ovine hearts had a single SPM and 2 hearts had 2 SPMs. In contrast, 4 canine hearts had a single SPM and 6 hearts had 3 or more SPMs. Additionally, only 2 porcine hearts had a single SPM, 4 hearts had 2 SPMs, and 4 hearts had 3 or more SPMs. Three human hearts had a single SPM, 3 hearts had 2 SPMs, and 2 hearts had 3 SPMs. All hearts from all species had other small papillary muscles on the septal wall which were not fully formed and projected into the right ventricle, as well as chordae appearing to attach directly to the septal wall.

In the left ventricle, all animal hearts from all species had a single APM with varying numbers of heads. In contrast, 5 human hearts had a single APM, 1 heart had 2 APMs, and 2 hearts had 3 APMs. All porcine and canine hearts had a single PPM in the left ventricle, while 8 ovine hearts had a single PPM and 2 hearts had 2 PPMs. Four human hearts had a single PPM in the left ventricle, and 4 hearts had 2 PPMs.

Generally, the right ventricle and left ventricle apexes of human hearts were far more trabeculated as compared to each species of animal hearts. In the right ventricle, the canine hearts were more trabeculated than those of porcine and ovine hearts. In contrast, the degree of trabeculation in the left ventricular apexes was similar across animal hearts. It was also noted that the epicardia of the ovine hearts were typically covered in greater amounts of fatty tissue relative to the canine and porcine hearts.

The shape of the ostia of the superior vena cavae and the inferior vena cavae was circular in all hearts examined, with the exception of 1 human heart in which the inferior vena cava ostium was removed during heart removal. The shape of the tricuspid valves and mitral valves ranged within species and

included elliptical, circular, nearly circular, and half-moon. Similarly, the aortic and pulmonary valves were circular in all hearts examined. The coronary sinus ostia were elliptical in the majority of hearts.

Due to cannulation of the hearts for perfusion and dissection of the pulmonary veins near the left atrium, the number of pulmonary veins could not be reliably determined in all hearts. Typically, major ostia were seen within each heart, but bifurcation patterns were different within and between species. Oftentimes, the myocardium traveled deep into the "vein" which was defined by a major ostium, yet the veins could be bifurcated almost directly at the myocardial/venous tissue junction into 2 to 4 veins. The canine hearts were the only exception to this generalization, in which 7 hearts had greater than 5 pulmonary veins (range 5–8).

6.4.3.2 Quantitative Comparisons

In general, calculated dimensions and heart weights were not well correlated, with the highest correlations found in ovine hearts. Therefore, statistical analyses were performed on both raw measurements and on those normalized to heart weight values. Statistically significant differences between the species were found for both raw and normalized data. Although some overlap of statistically significant differences existed between the raw and normalized values, oftentimes statistical significance was not conserved between the two methods. Therefore, only raw data is presented throughout the remaining portion of this chapter and in Tables 6.4 and 6.5, with statistically significant differences noted.

Externally, the average anterior (anterosuperior) base to apex distance was significantly longer in sheep hearts than canine hearts. The average base to apex distance on the posterior (posteroinferior) and left lateral aspects was significantly longer in the human hearts than swine, canine, and ovine hearts. The average right lateral base to apex distance was significantly longer in human hearts compared to swine and canine hearts, and the ovine hearts were also significantly longer than the swine hearts. The average external length of the coronary sinus was significantly longer in the human hearts compared to the swine, canine, and ovine hearts (Table 6.4).

Internally, the average superior (posterolateral) to inferior (anteroseptal) coronary sinus ostium diameter was significantly larger in human hearts compared to swine, canine, and ovine hearts. The average lateral (inferior) to septal (superior) diameter was significantly smaller in canine hearts compared to human, swine, and ovine hearts. As stated earlier, Thebesian valves were present in all human hearts. Due to this valve, the functional ostium of the coronary sinus (i.e., that which was not covered by a Thebesian valve) was reduced in the superior/inferior dimension in these hearts as the attachment of the valve was typically in the posterolateral/anteroseptal direction. When taking into account the Thebesian valve, the average diameter of the functional ostium of the human hearts was significantly smaller than that of the swine and ovine hearts (Table 6.5).

The average tricuspid valve diameters were all of similar size, with the exception of the anterior (superior) to posterior (inferior) dimension, which was significantly larger in human hearts than pig hearts. The average right ventricular inflow tract length was significantly longer in human hearts compared to the animal hearts in all dimensions analyzed. No significant differences were seen in the average length of the outflow tracts of the right ventricles, with the exception of the mid-left cusp to apex dimension, which was significantly shorter in canine hearts than human hearts. The average diameter of the sinotubular junction of the pulmonic trunk was significantly greater in the human hearts as compared to the animal hearts. No significant differences were observed in the average diameters of the basal annular ring of the pulmonic valve (Table 6.5).

No significant differences were observed in the average diameter of mitral valve in the anterior (superior) to posterior (inferior) dimension. However, the average diameter of the mitral valve in the septal (posterior) to lateral (anterior) dimension was significantly larger in the human hearts as compared to the animal hearts. The average dimensions of the inflow tracts of the left ventricle were significantly shorter in the canine hearts compared to human, swine, and ovine hearts in all dimensions analyzed. The average diameter of the left ventricular outflow tract was generally longer in the human hearts than the animal hearts. The average

Table 6.4 External dimensions (mean ± std. dev)

Measurement	Human	Swine	Canine	Ovine
Anterior (anterosuperior) base to apex distance (mm)	98.7 ± 14.6	101.2 ± 6.8	93.5 ± 4.1	111.1 ± 16.8 **ζ**
Posterior (posteroinferior) base to apex distance (mm)	87.7 ± 12.4	65.6 ± 4.2	71.3 ± 2.9	72.6 ± 7.6 **αβθ**
Right lateral base to apex distance (mm)	106.4 ± 10.9	88.4 ± 4.8	94.3 ± 5.8	103.8 ± 12.7 **αβε**
Left lateral base to apex distance (mm)	99.7 ± 9.5	80.8 ± 5.3	78.6 ± 3.5	87.4 ± 10.2 **αβθ**
Coronary sinus length	46.5 ± 5.2	25.1 ± 2.7	29.8 ± 6.7	29.9 ± 8.6 **αβθ**

Significant differences are noted by the following symbols: α—human, swine; β—human, canine; θ—human, ovine; δ—swine, canine; ε—swine, ovine; ζ—canine, ovine

Table 6.5 Internal dimensions (mean ± std. dev)

Measurement	Human	Swine	Canine	Ovine
Coronary sinus ostium				
CS Os superior (posterolateral) to inferior (anteroseptal) diameter (mm)	12.3 ± 4.2	7.7 ± 1.4	5.0 ± 1.0	8.1 ± 3.2 **αβθ**
CS Os lateral (inferior) to septal (superior) diameter (mm)	15.7 ± 2.4	16.4 ± 2.9	9.8 ± 2.2	18.3 ± 5.0 **βδζ**
CS Os functional ostium—Thebesian valve to opposite edge diameter (mm)	8.1 ± 2.9	NA	NA	NA **αθδζ**
Tricuspid valve				
Tricuspid valve anterior (superior) to posterior (inferior) diameter (mm)	43.0 ± 3.1	37.2 ± 4.2	38.8 ± 3.0	39.9 ± 3.8 **α**
Tricuspid valve septal (posterior) to lateral (anterior) diameter	37.7 ± 7.2	30.3 ± 5.5	29.5 ± 4.6	36.0 ± 9.4
RV inflow tract				
Tricuspid valve anterior (superior) to RV apex distance (mm)	86.9 ± 12.9	72.0 ± 4.7	65.3 ± 4.1	66.1 ± 15.9 **αβθ**
Tricuspid valve posterior (inferior) to RV apex distance (mm)	78.9 ± 19.9	55.5 ± 3.3	49.3 ± 3.6	51.9 ± 11.1 **αβθ**
Tricuspid valve septal (posterior) to RV apex distance (mm)	77.4 ± 14.0	61.8 ± 4.3	55.5 ± 4.8	59.5 ± 10.1 **αβθ**
Tricuspid valve lateral (anterior) to RV apex distance (mm)	83.7 ± 21.0	61.6 ± 4.9	55.7 ± 3.8	58.7 ± 16.7 **αβθ**
Tricuspid valve center to RV apex distance (mm)	73.1 ± 19.2	51.8 ± 2.7	45.7 ± 4.5	50.4 ± 9.8 **αβθ**
Pulmonic valve				
Pulmonic valve sinotubular junction diameter (mm)	28.1 ± 3.8	18.7 ± 1.6	18.3 ± 3.3	22.8 ± 5.7 **αβθ**
Pulmonic valve basal annular diameter (mm)	31.1 ± 3.2	25.6 ± 2.0	25.5 ± 2.9	29.8 ± 6.8
RV outflow tract				
Pulmonic valve mid-anterior cusp pulmonic valve to apex distance (mm)	86.9 ± 14.7	93.3 ± 6.2	84.8 ± 5.0	90.4 ± 16.0
Pulmonic valve mid-right cusp pulmonic valve to apex distance (mm)	93.9 ± 15.0	85.4 ± 5.9	76.7 ± 4.1	82.4 ± 21.1
Pulmonic valve mid-left cusp pulmonic valve to apex distance (mm)	87.9 ± 13.6	79.0 ± 4.7	69.4 ± 4.3	79.2 ± 9.7 **β**
Pulmonic valve center pulmonic valve to apex distance (mm)	90.4 ± 16.7	85.6 ± 6.5	77.9 ± 4.3	81.4 ± 11.3
Mitral valve				
Mitral valve anterior (superior) to posterior (inferior) diameter (mm)	37.9 ± 4.6	31.0 ± 3.9	31.3 ± 4.6	36.9 ± 7.4
Mitral valve septal (posterior) to lateral (anterior) diameter (mm)	32.5 ± 5.6	23.7 ± 2.7	22.0 ± 4.9	25.8 ± 6.3 **αβθ**
LV inflow tract				
Mitral valve anterior (superior) to LV apex distance (mm)	83.7 ± 18.0	76.8 ± 6.3	63.1 ± 6.0	75.7 ± 13.5 **β**
Mitral valve posterior (inferior) to LV apex distance (mm)	78.2 ± 18.2	68.2 ± 5.5	60.0 ± 5.8	67.4 ± 11.6 **β**
Mitral valve septal (posterior) to LV apex distance (mm)	80.7 ± 15.7	70.6 ± 6.1	65.2 ± 5.8	70.2 ± 13.4 **β**
Mitral valve lateral (anterior) to LV apex distance (mm)	77.4 ± 17.3	72.1 ± 5.3	59.4 ± 4.8	72.1 ± 13.2 **β**
Mitral valve center to LV apex distance (mm)	69.5 ± 16.2	62.0 ± 5.9	52.1 ± 4.9	62.3 ± 11.3 **β**
Aortic valve				
Aortic valve sinotubular junction diameter (mm)	26.4 ± 3.0	21.4 ± 2.3	16.8 ± 2.7	20.4 ± 3.8 **αβθδ**
Aortic valve basal annular diameter (mm)	30.0 ± 2.6	25.1 ± 3.2	23.2 ± 4.1	28.9 ± 5.4 **βζ**
LV outflow tract				
Aortic valve mid-right coronary cusp to LV apex distance (mm)	89.9 ± 18.6	72.5 ± 6.2	65.2 ± 5.8	76.2 ± 13.3 **αβ**
Aortic valve mid-left coronary cusp to LV apex distance (mm)	89.7 ± 18.6	77.1 ± 5.5	67.1 ± 6.1	77.3 ± 14.5 **β**
Aortic valve mid-non-coronary cusp to LV apex distance (mm)	92.7 ± 20.1	73.8 ± 6.2	67.1 ± 7.1	73.0 ± 11.9 **αβθ**
Aortic valve center to LV apex distance (mm)	90.8 ± 18.3	75.9 ± 5.8	63.7 ± 6.6	75.2 ± 12.8 **βθ**

Significant differences are noted by the following symbols: α—human, swine; β—human, canine; θ—human, ovine; δ—swine, canine; ε—swine, ovine; ζ—canine, ovine

human dimensions were significantly longer than the swine and canine hearts in the mid-right cusp dimension, significantly longer than the canine hearts in the mid-left dimension, significantly longer than all hearts in the non-coronary dimension, and significantly longer than the canine and ovine hearts from the center of the aortic valve. The average diameter of the sinotubular junction of the aorta was significantly larger in the human hearts than all animal hearts. Additionally, the average diameter of the swine hearts was significantly longer than the canine hearts at this location. Finally, the average diameter of the basal annulus of the aortic valve was significantly larger in human and ovine hearts than canine hearts (Table 6.5).

6.4.4 Discussion and Consideration of Previous Studies on Comparative Anatomy

In the present study, we examined the gross morphology of the hearts of humans, pigs, dogs, and sheep and compared them both qualitatively and quantitatively. To the authors' knowledge, this is the first study specifically aimed at elucidating both qualitative and quantitative similarities and/or differences in the cardiac anatomy of these commonly employed species for cardiovascular research. These presented findings should be seen as a unique initial database on the overall shape of hearts, appendages, and valves, the presence or absence of specific anatomical features, and quantitative dimensions, which were measured in nondissected pressure-fixed, end-diastolic volume hearts. These comparisons demonstrate that important anatomical differences exist between hearts isolated from humans, pigs, dogs, and sheep. Hopefully, these results can be used by future investigators as an aid in making critical choices as to which animal model would be best for their specific biomedical/cardiovascular research.

A sizeable quantity of literature has been published on many qualitative aspects of large mammalian cardiac anatomy. However, much of this research is very general (i.e., all mammalian hearts have a right and left atrial appendage) [11, 13, 14, 25] or very specific (i.e., comparative cardiac anatomy of the cardiac foramen ovale) [50], and, importantly, most research is not done in a truly comparative fashion. Furthermore, much of this literature does not provide information useful for those specifically performing cardiovascular research with the hope of translating such results to relevant human research.

There are specific examples of anatomical structure that we studied in these comparative analyses that have been described somewhat differently in the previous literature. Crick et al. [13] reported that the shape of the porcine heart was valentine; we observed this shape in 8 of 10 hearts. They also reported a trapezoidal shape of the human hearts they examined. Greater variability was seen in the observed shape of our human hearts with no general trend seen. The formation of the apex of the heart entirely by the left ventricle has also been previously reported for all animals examined in this study [12–14]; this is also the case for most of the human hearts in this study and is widely reported in literature and textbooks. The presence of a moderator band in the right ventricle in all hearts examined has also been previously noted [11, 13, 51]. However, Truex and Warshaw [26], while finding a moderator band in the right ventricle of all sheep and pigs studied, failed to find such a band in the canine hearts they examined and only found a band in 56.8 % of human hearts. This discrepancy was likely due to definition and to the different morphology presented by the band in these animals. Interestingly, we observed left ventricular bands in nearly all of the hearts examined (7 human, 9 swine, 10 canine, and 10 ovine). Gerlis et al. [27] reported that they found left ventricular bands in 100 % of ovine hearts ($n=42$), 100 % of canine hearts ($n=12$), and 86 % of porcine hearts they examined ($n=36$), but only in 52 % of adult hearts examined ($n=50$). Joudinaud and colleagues [51] cataloged the papillary muscles of the swine heart in 2006, classifying them based on the leaflets they supported. They defined them as anteroposterior (APM in this study), anteroseptal (SPM in this study), and posteroseptal (PPM in this study). They found, on average, 1.1 anteroposterior papillary muscles, 2.4 posteroseptal papillary muscles, and 1.8 anteroseptal papillary muscles. These findings are similar to our observations of an average of 1 APMs, 1.9 PPMs, and 2.1 SPMs, with a slightly different weighting toward more SPMs than PPMs in our study compared to their research. While a specific report on the number of papillary muscles in the ventricles of other hearts could not be found, it has been reported that human, canine, porcine, and ovine hearts typically have three papillary muscles (APM, PPM, and SPM) in the right ventricle and two (APM and PPM) in the left ventricle [11]. While our findings are similar for the left ventricle, we found a much greater variability in the number of papillary muscles in the right ventricle of all species examined, with some canine hearts having as many as 6 right ventricular papillary muscles.

Relative to recent interest in the development of access and closure devices for the atrium or means for occluding the left atrial appendage in patients with atrial fibrillation, it should be noted that some of our qualitative findings were different from what has been previously reported. For example, Crick et al. [13] reported that the right atrial appendages of the swine hearts typically had a tubular shape, while we found that the right atrial appendages were shaped more like a half-moon. Also, they reported that the right and left atrial appendages of swine hearts were of similar size; we found that the left atrial appendages were larger in 90 % of the hearts examined. This discrepancy could be related to the breed differences; Crick et al. did not provide the specific

breed of the animals used in their study. Interestingly, they reported that the right atrial appendages of the human hearts were "appreciably" larger than the left, a finding which is similar to our findings in 3 of the 8 hearts examined. It should be noted that we believe the authors of that study were referring to the free portion of the right appendage for comparison, as it is believed that the atrial appendage of the right atrium technically includes all pectinate portions of the atrium arising from the terminal crest [52]. However, the authors reference that the appendage on the right side consists of pectinate muscles and that these pectinate muscles "surround entirely the parietal margin of the vestibule of the tricuspid valve." If the definition is used to describe the right atrial appendage, one would find that only in rare cases (most likely pathological) would the left atrial appendage be larger than the right as the pectinate muscles of the left atrium are nearly always contained within the free portion.

As mentioned previously, there has been a lack of published information comparing canine, porcine, and ovine hearts quantitatively. Yet, Lev et al. [53] eloquently described methods to study the congenitally malformed heart quantitatively in 2D in 1961 and followed with an excellent paper on the anatomy of the normal human child heart in 1963 [54]. These methods were applied to the swine heart in a publication by Eckner et al. [55]. More specifically, they measured the inflow and outflow tracts of the swine right and left ventricle using methods as described by Lev et al. in 1961. From 27 porcine hearts weighing in the range of 200–300 g, they found the length of the right ventricular inflow tract to be 5.4 ± 0.4 cm, the length of the right ventricular outflow tract to be 8.6 ± 0.5 cm, the length of the left ventricular inflow tract to be 7.6 ± 0.4 cm, and the length of the left ventricular outflow tract to be 7.4 ± 0.4. In the present study, we found the length of the right ventricular inflow tract to be 5.6 ± 0.3 cm, the right ventricular outflow tract to be 7.9 ± 0.5 cm, the length of the left ventricular inflow tract to be 6.8 ± 0.6 cm, and the length of the left ventricular outflow tract to be 7.3 ± 0.6 cm. Overall, the measurements from the two studies are similar; however, the right ventricular outflow tract and left ventricular inflow tract were noticeably shorter in the hearts examined in this study compared to those of Eckner et al. It should be noted that the methods described by Lev et al. and used by Eckner et al. were slightly ambiguous regarding their definitions of the measurement end points. For instance, the right ventricular inflow tract measurement was described as "the length of the inflow tract of the right ventricle is measured from a point at the tricuspid annulus in the center of the posterior wall to the apex" [53]. Thus, depending on one's interpretation of the location of this point, significantly varied measurements could be obtained. In spite of this, the measurement locations in the present study were selected so that they were as close as possible to as those measured by Eckner et al. Similarly, another group of investigators, Alvarez et al. [56], applied similar assessment methods to the right ventricles of 75 porcine hearts. They found the length of the right ventricular inflow tract was on average 5.9 ± 0.8 cm, and the outflow tract was 8.4 ± 1.0 cm. Interestingly, the outflow tract length was again longer than that measured in the current study, while the inflow tract length was similar among all three studies. While the breed of swine used by Eckner et al. was not reported, Alvarez et al. used hearts obtained from the Europa breed. The hearts used in the present study were from Yorkshire cross animals; this variation in breed may explain the differences in measured dimensions.

In contrast to the lack of publications examining the gross dimensions of the hearts, there have been publications concerned with the dimensions of the cardiac valves, mostly focused on the aortic and mitral valves. The sheep is the most common model used in experimental models of mitral regurgitation, and, due to this, there are numerous studies examining both the normal and pathological anatomy of the mitral valve (see also Chap. 27). Yet, many of these studies do not provide comparable measurements. However, in 1997, Gorman et al. published a study of 6 sheep, demonstrating that the end-diastolic anterior–posterior dimension was 26.6 mm and the end-diastolic commissure–commissure dimension was 35.4 mm [57]. In 2002, Timek et al. reported, in a study of 6 sheep instrumented with radiopaque markers, that the end-diastolic anterior–posterior dimension of the mitral valve was 2.6 ± 0.3 cm and the end-diastolic commissure–commissure dimension was 3.6 ± 0.4 cm [58]. While the nomenclature used between these studies and the data we presented is slightly different, these reported measurements are very similar overall: our measurements were 25.8 ± 6.3 mm septal–lateral (anterior–posterior) and 36.9 ± 7.4 mm anterior–posterior (superior–inferior or commissure–commissure). Tsakiris et al. [59] reported that the average early diastolic anterior–posterior dimension of 5 canine hearts was 2.1 ± 0.2 cm, similar to our findings of 22.0 ± 4.9 mm. Chandraratna and Aronow [60] reported a mean maximal diastolic anterior–posterior diameter of 2.2 ± 0.2 cm and end-systolic anterior–posterior diameter of 1.8 ± 0.2 cm from 23 normal human subjects studied with echocardiography. Nordblom and Bech-Hanssen [61] reported a mean end-diastolic anterior–posterior dimension of 2.9 ± 0.4, mean end-systolic anterior–posterior dimension of 3.3 ± 0.3 cm, and mean end-diastolic commissure–commissure dimension of 3.7 ± 0.4 cm in 38 normal human subjects. These two publications show the wide variation of reported results in the literature. Reporting on all of the mitral publications is beyond the scope of this paper; however, it should be noted that our results were more similar to the publication by Nordblom than that of Chandraratna. Added considerations in comparing anatomical studies that one needs to keep in mind are that differing methodologies may slightly

skew data or that newer methodologies may provide more accurate measurements. For example, this could be due to changes in the definition of the dimensions measured and also to higher resolution offered by newer ultrasound technology which provides important in vivo measurements.

Regarding the aortic valve, Sands et al. published the only available quantitative study examining the aortic valves of multiple hearts, including 10 swine, 9 ovine, 9 bovine, and 7 humans [30]. Interestingly, in their investigations, aortic valve diameters were measured via passing an obturator through fresh hearts until a snug fit was determined. They reported the average annulus diameters of 26.4 ± 3.2 mm in human hearts, 26.6 ± 1.8 mm in pig hearts, and 25.8 ± 0.3 mm in sheep hearts. It may be assumed that, by annulus, they were actually referring to the basal portion of the annulus. For the in vitro data on perfusion-fixed hearts we provided above, larger average basal annular diameters in human hearts (30.0 ± 2.6 mm) and in sheep hearts (28.9 ± 5.4 mm) were observed, and slightly smaller average diameters in pig hearts (25.1 ± 3.2 mm) were found. More recently, Lansac and colleagues published a sonometric study of 8 ovine aortic valves and ascending aortas, in which they reported average basal annular diameters of 20.7 ± 0.4 mm and commissure diameters of 14.1 ± 0.2 mm, which are both smaller than our reported diameters [62]. Sim and colleagues [63] published a comparison of 12 human and 12 swine aortic valves in which they reported mean diameters of 2.6 ± 0.1 cm for human hearts ($n = 12$) and 2.2 ± 0.3 cm for swine hearts, both which are smaller than that observed in our studies. Interestingly, Swanson and Clark [64] published a study of 5 normal human aortic valves in 1974, using silicone casts of aortic valves prepared at various pressures (0–120 mmHg). Regardless of the pressure used, on average, the basal annulus in their study was smaller than that observed in this study. Finally, in support of the fact that sheep are the most commonly used animal model for aortic valve studies, we found that the average basal annulus diameters were most similar between sheep and human hearts. However, we noted that the sinotubular junction diameters were significantly smaller in all animals studied as compared to the human hearts. This could have implications for selection of an animal model for newer technologies such as transcatheter-delivered aortic valves, as some technology engages the sinotubular junction for fixation of the device.

Publications on the valves on the right side of the heart are scarce, especially the pulmonic valve, and none were found with comparable measurements. The tricuspid valve has been quantitatively studied in sheep, canines, and humans, although like mitral valve studies, similar measurements to this study are not evident in many publications. Jouan and colleagues [65] studied the tricuspid annulus of 7 sheep and showed that during the cardiac cycle the minimum diameter (approximately perpendicular to the septum) changed from 17.8 ± 1.9 to 21.2 ± 2.0 mm and maximum diameter (approximately parallel to the septum) changed from 36.4 ± 2.4 to 40.1 ± 2.6 mm. While this report does not specifically give orientational references for these numbers, the minimum diameter is described as perpendicular to the septum and therefore is much smaller than that observed in this study. The maximum diameter, however, is similar to the anterior–posterior (superior–inferior) diameter of this study. In 2007, Anwar and colleagues reported the average tricuspid annular diameter of 100 normal patients to be 4.0 ± 0.7 cm [66]. Again, no orientational references were given to this diameter, but rather it appears to be the maximal diameter, which most likely correlates to the anterior–posterior (superior–inferior) diameter of this study with similar values observed.

The dimensions analyzed in the perfusion-fixed hearts we provided above can also be used to illustrate some differences in gross morphology. Interestingly, the average right ventricular inflow tract of the human hearts examined in this study was significantly longer than that of the other hearts examined, although the outflow tracts of the right ventricles were relatively the same length among all hearts. This has direct applicability to right ventricular apical pacemaker lead design, in which the designs intended ultimately for human hearts are studied in any of the animal species examined in this study—the lead length to reach the right ventricular apex from the tricuspid valve in the animal species is on average 1–2 cm shorter than in human hearts. The rest of the implant anatomy would also need to be considered for complete analysis. Another interesting finding was the significantly smaller diameter of the coronary sinus ostia in canine hearts compared to the other hearts examined. Coupled with the external measured length of the coronary sinus, which was significantly longer in human hearts than other hearts, implications for animal model selection in biomedical device research become obvious. Similar to the right ventricular apical lead length mentioned above, coronary venous-delivered left ventricular pacing lead lengths may need to be shortened for animal work. Furthermore, when choosing an animal model to simulate coronary sinus access similar to humans with Thebesian valves, the canine model becomes an obvious choice due to the similarity in size. Maric et al. [67] examined the diameter of the coronary sinus ostium in humans and dogs; they found the diameter to be 8.4 ± 2.6 mm in humans and 6.5 ± 1.3 mm in dogs. Unfortunately, Maric does not mention which diameter was measured (superior/inferior or lateral/septal).

6.5 Summary

Cardiac research is an important field that will continue to thrive for many years. It is critical that the appropriate animal models are employed to perform well-designed translational research prior to human clinical trials. In this chapter, we

presented a unique set of comparative information relative to cardiac anatomy of several large mammalian models commonly used for such laboratory testing: the pig, dog, and sheep. Important difference and similarities exist that may impact research results relative to either device testing or pharmacological therapeutic trials. The novel research data presented here from our laboratory were specifically designed to systematically compare the anatomical features of these animal models to humans, both qualitatively and quantitatively. The techniques employed were unique in that they allowed study of nondissected hearts, providing measurements from realistic geometric configurations. We observed that specific differences in the cardiac anatomy exist between the species, for hearts isolated and pressure perfusion fixed with similar weights, and that these differences may be useful in choosing an animal model for certain types of biomedical research. It is likely as CT and MRI methodologies continue to advance that more specific structural comparisons can be performed on functioning hearts, yet details about animal age, weight, health status, and/or breed will need to be well described in order to make such data sets of higher value.

References

1. Paul EF, Paul J (2001) Why animal experimentation matters: the use of animals in medical research. Social Philosophy and Policy Foundation: Transaction, New Brunswick
2. Monamy V (ed) (2000) Animal experimentation: a guide to the issues. Cambridge University Press, Cambridge/New York
3. Nutton V (2002) Portraits of science. Logic, learning, and experimental medicine. Science 295:800–801
4. Persaud TVN (ed) (1997) A history of anatomy: the post-Vesalian era. Charles C Thomas Publisher, Springfield
5. Hearse DJ (2000) The elusive coypu: the importance of collateral flow and the search for an alternative to the dog. Cardiovasc Res 45:215–219
6. Christensen GC, Campeti FL (1959) Anatomic and functional studies of the coronary circulation in the dog and pig. Am J Vet Res 20:18–26
7. Hughes HC (1986) Swine in cardiovascular research. Lab Anim Sci 36:348–350
8. Kong Y, Chen JT, Zeft HJ et al (1969) Natural history of experimental coronary occlusion in pigs: a serial cineangiographic study. Am Heart J 77:45–54
9. Verdouw PD, van den Doel MA, de Zeeuw S et al (1998) Animal models in the study of myocardial ischaemia and ischaemic syndromes. Cardiovasc Res 39:121–135
10. Getty R (1975) General heart and blood vessels. In: Getty R (ed) Sisson and Grossman's the anatomy of the domestic animals, 5th edn. Saunders, Philadelphia, pp 164–175
11. Michaëlsson M, Ho SY (eds) (2000) Congenital heart malformations in mammals: an illustrated text. Imperial College Press, London/River Edge
12. Ghoshal NG (1975) Ruminant, carnivore, porcine: heart and arteries. In: Sisson S, Grossman JD, Getty R (eds) Sisson and Grossman's: the anatomy of the domestic animals, 5th edn. Saunders, Philadelphia, pp 960–1023, 1594–1651, 1306–1342
13. Crick SJ, Sheppard MN, Ho SY et al (1998) Anatomy of the pig heart: comparisons with normal human cardiac structure. J Anat 193:105–119
14. Evans HE (1993) The heart and arteries. In: Miller ME, Evans HE (eds) Miller's anatomy of the dog, 3rd edn. Saunders, Philadelphia, pp 586–602
15. Netter FH (ed) (1979) Heart. Ciba Pharmaceutical Company. Medical Education Division. The Division, West Caldwell
16. Holt JP, Rhode EA, Kines H (1968) Ventricular volumes and body weight in mammals. Am J Physiol 215:704–715
17. Lee JC, Taylor FN, Downing SE (1975) A comparison of ventricular weights and geometry in newborn, young, and adult mammals. J Appl Physiol 38:147–150
18. Holt JP (1970) The normal pericardium. Am J Cardiol 26:455–465
19. Naimark WA, Lee JM, Limeback H et al (1992) Correlation of structure and viscoelastic properties in the pericardia of four mammalian species. Am J Physiol 263:H1095–H1106
20. Spodick DH (ed) (1997) The pericardium: a comprehensive textbook. M. Dekker, New York
21. Moore T, Shumacker HJ (1953) Congenital and experimentally produced pericardial defects. Angiology 4:1–11
22. Elias H, Boyd L (1960) Notes on the anatomy, embryology and histology of the pericardium. J N Y Med Coll 2:50–75
23. Hurst JW (ed) (1988) Atlas of the heart. McGraw-Hill: Gower Medical Pub, New York
24. Montagna W (ed) (1959) Comparative anatomy. Wiley, New York
25. Kent GC, Carr RK (eds) (2001) Comparative anatomy of the vertebrates, 9th edn. McGraw Hill, Boston
26. Truex RC, Warshaw LJ (1942) The incidence and size of the moderator band in man and mammals. Anat Rec 82:361–372
27. Gerlis LM, Wright HM, Wilson N et al (1984) Left ventricular bands. A normal anatomical feature. Br Heart J 52:641–647
28. Quill JL, Hill AJ, Laske TG, Alfieri O, Iaizzo PA (2009) Mitral leaflet anatomy revisited. J Thorac Cardiovasc Surg 137:1077–1081
29. Walmsley R (1978) Anatomy of human mitral valve in adult cadaver and comparative anatomy of the valve. Br Heart J 40:351–366
30. Sands MP, Rittenhouse EA, Mohri H et al (1969) An anatomical comparison of human pig, calf, and sheep aortic valves. Ann Thorac Surg 8:407–414
31. Ansari A (2001) Anatomy and clinical significance of ventricular Thebesian veins. Clin Anat 14:102–110
32. Pina JAE, Correia M, O'Neill JG (1975) Morphological study on the Thebesian veins of the right cavities of the heart in the dog. Acta Anat 92:310–320
33. Ruengsakulrach P, Buxton BF (2001) Anatomic and hemodynamic considerations influencing the efficiency of retrograde cardioplegia. Ann Thorac Surg 71:1389–1395
34. Weaver ME, Pantely GA, Bristow JD et al (1968) A quantitative study of the anatomy and distribution of coronary arteries in swine in comparison with other animals and man. Cardiovasc Res 20:907–917
35. Anderson RH, Becker AE (eds) (1992) The heart: structure in health and disease. Gower Medical Pub, London/New York
36. Kloner RA, Ganote CE, Reimer KA et al (1975) Distribution of coronary arterial flow in acute myocardial ischemia. Arch Pathol 99:86–94
37. Koke JR, Bittar N (1978) Functional role of collateral flow in the ischaemic dog heart. Cardiovasc Res 12:309–315
38. Redding VJ, Rees JR (1968) Early changes in collateral flow following coronary artery ligation: the role of the sympathetic nervous system. Cardiovasc Res 2:219–225
39. Weisse AB, Kearney K, Narang RM et al (1976) Comparison of the coronary collateral circulation in dogs and baboons after coronary occlusion. Am Heart J 92:193–200

40. Schaper W, Flameng W, De Brabander M (1972) Comparative aspects of coronary collateral circulation. Adv Exp Med Biol 22:267–276
41. Gregg D, Shipley R (1947) Studies of the venous drainage of the heart. Am J Physiol 151:13–25
42. Patek PP (1939) The morphology of the lymphatics of the mammalian heart. Am J Anat 64:203–249
43. Johnson RA, Blake TM (1966) Lymphatics of the heart. Circulation 33:137–142
44. Symbas PN, Cooper T, Gantner GEJ et al (1963) Lymphatic drainage of the heart: effect of experimental interruption of lymphatics. Surg Forum 14:254–256
45. Anderson RH, Becker AE, Brechenmacher C et al (1975) The human atrioventricular junctional area. A morphological study of the A-V node and bundle. Eur J Cardiol 3:11–25
46. Bharati S, Levine M, Huang SK et al (1991) The conduction system of the swine heart. Chest 100:207–212
47. Frink RJ, Merrick B (1974) The sheep heart: coronary and conduction system anatomy with special reference to the presence of an os cordis. Anat Rec 179:189–200
48. Ho SY, Kilpatrick L, Kanai T et al (1995) The architecture of the atrioventricular conduction axis in dog compared to man: its significance to ablation of the atrioventricular nodal approaches. J Cardiovasc Electrophysiol 6:26–39
49. Hearse DJ, Sutherland FJ (2000) Experimental models for the study of cardiovascular function and disease. Pharmacol Res 41:597–603
50. Macdonald AA, Johnstone M (1995) Comparative anatomy of the cardiac foramen ovale in cats (Felidae), dogs (Canidae), bears (Ursidae) and hyaenas (Hyaenidae). J Anat 186:235–243
51. Joudinaud TM, Flecher EM, Duran CM (2006) Functional terminology for the tricuspid valve. J Heart Valve Dis 15:382–388
52. Anderson RH, Cook AC (2007) The structure and components of the atrial chambers. Europace 9:vi3–vi9
53. Lev M, Rowlatt UF, Rimoldi HJ (1961) Pathologic methods for the study of the congenitally malformed heart. AMA Arch Pathol 72:493–511
54. Rowlatt UF, Rimoldi HJ, Lev M (1963) The quantitative anatomy of the normal child's heart. Pediatr Clin N Am 10:499–588
55. Eckner FA, Brown BW, Overll E et al (1969) Alteration of the gross dimensions of the heart and its structures by formalin fixation. A quantitative study. Virchows Arch A Pathol Pathol Anat 346:318–329
56. Alvarez L, Rodriquez JE, Saucedo R et al (1995) Swine hearts: quantitative anatomy of the right ventricle. Anat Histol Embryol 24:25–27
57. Gorman JH 3rd, Gorman RC, Jackson BM et al (1997) Distortions of the mitral valve in acute ischemic mitral regurgitation. Ann Thorac Surg 64:1026–1031
58. Timek TA, Lai DT, Tibayan F et al (2002) Atrial contraction and mitral annular dynamics during acute left atrial and ventricular ischemia in sheep. Am J Physiol Heart Circ Physiol 283:H1929–H1935
59. Tsakiris AG, Padiyar R, Gordon DA et al (1977) Left atrial size and geometry in the intact dog. Am J Physiol 232:H167–H172
60. Chandraratna PA, Aronow WS (1981) Mitral valve ring in normal vs dilated left ventricle. Cross-sectional echocardiographic study. Chest 79:151–154
61. Nordblom P, Bech-Hanssen O (2007) Reference values describing the normal mitral valve and the position of the papillary muscles. Echocardiography 24:665–672
62. Lansac E, Lim HS, Shomura Y et al (2002) A four-dimensional study of the aortic root dynamics. Eur J Cardiothorac Surg 22:497–503
63. Sim EK, Muskawad S, Lim CS et al (2003) Comparison of human and porcine aortic valves. Clin Anat 16:193–196
64. Swanson M, Clark RE (1974) Dimensions and geometric relationships of the human aortic valve as a function of pressure. Circ Res 35:871–882
65. Jouan J, Pagel MR, Hiro ME et al (2007) Further information from a sonometric study of the normal tricuspid valve annulus in sheep: geometric changes during the cardiac cycle. J Heart Valve Dis 16:511–518
66. Anwar AM, Geleijnse ML, Soliman OI et al (2007) Assessment of normal tricuspid valve anatomy in adults by real-time three-dimensional echocardiography. Int J Cardiovasc Imaging 23:717–724
67. Maric I, Bobinac D, Ostojic L et al (1996) Tributaries of the human and canine coronary sinus. Acta Anat (Basel) 156:61–69